Ultraviolet Spectra and Geometric Albedos of 45 Asteroids

E.E. Roettger*
Jet Propulsion Laboratory
4800 Oak Grove Drive
Pasadena, CA 91109

and

B.J. Buratti

Jet Propulsion Laboratory
Mail Code 183-501
4800 Oak Grove Drive
Pasadena, CA 91109
818-354-7427
fax: 818-354-0966
internet: buratti@jplpds.jpl.nasa.gov

Submitted to Icarus
16 May 1994
Revised
5 August 1994

18 'pages of manuscript, 2 tables, 6 figures

*Current Address:
The Adler Planetarium
1300 South Lake Shore Drive
Chicago, 11.60130
312-322-0338
fax: 312-322-2257
eroettge@midway.uchicago.edu

Proposed running head:

UV Spectra of 45 Asteroids

Direct correspondence to:

B. Buratti
Jet Propulsion Laboratory
4800 Oak Grove Dr.
MS 183-501
Pasadena, CA 91109

818-354-7427
fax: 818-354-0966
internet: buratti@jplpds.jpl.nasa.gov

Abstract

Spectral reflectances and geometric albedos between 2300 and 3250 Å are determined for 45 asteroids from data acquired by the international Ultraviolet Explorer satellite. The. geometric albedos arc consistently low, ranging from -0.02 for C-type asteroids to -0.08 for M-type asteroids. An exception is the single L3-type asteroid (44 Nysa) with a geometric albedo of 0.3 at 2950 Å. We find that the three major asteroid taxonomic classes persist into the UV. The taxonomic classes arc distinguished primarily by their albedos, but S-types arc generally redder than C-or M-types. The first ultraviolet phase curves of asteroids arc presented.

1.1 ntroduction

Asteroids are a diverse group, both spectrally and dynamically; some even appear to be inactive comets (e.g., Weissman *et al.* 1989 and references therein). Connections have been drawn to meteorites (Binzel and Xu 1993) and other small solar system bodies (e.g., Stern *et al.* 1990). Asteroids are worthy of study because at least some are relatively pristine remnants of the primordial solar nebula, giving us clues to the formation and evolution of the solar system, and insight into other possible planetary systems.

The ultraviolet regime of the spectrum is a relatively unexplored frontier for studying asteroids. A few near-UV data points sometimes appear on the end of a visible spectrum (e.g., Tholen and Barucci 1989, McFadden *et al.* 1993). We would expect the ultraviolet to be potentially important regime for studies of asteroids, containing the spectral signature of primitive materials (e.g., Lee and Wdowiak 1993) and electronic charge transfer bands, and the unpredictable possibilities associated with the exploration of a new region of the spectrum.

Before the advent of the Hubble Space Telescope (HST), UV observations of asteroids were obtained by the international Ultraviolet Explorer (IUE) satellite. Of the 46 asteroids observed with IUE (through November 1992), spectra from fewer than two-thirds have been reduced in a uniform manner and published, although several focused studies of individual asteroids have been published (Festou *et al.* 1991, A'Hearn and Feldman 1992, Schultz *et al.* 1993)

Butterworth *et al.* (1980) and Butterworth and Meadows (1985) published spectra of 28 asteroids observed with the IUE. Since this work was accomplished, we have available significantly improved IUE calibrations, a more precise solar spectra, spectra of more objects, and additional spectra for objects already observed (some of which are high quality, due to better pointing techniques). Finally, we are able to construct ultraviolet phase curves and make solar phase angle corrections to accurately determine absolute fluxes . We are thus able to develop the first systematic and reliable study of asteroids in the ultraviolet, giving a much more secure determination of spectral geometric al bedo than previous attempts accomplished. One motivation for this study is to provide a solid basis for object selection and calculation of exposure times for ultraviolet observations with HST.

We present here ultraviolet spectra (2300-3300 Å) and geometric albedos (2670 Å) of 45 asteroids (data from one asteroid was not usable). The original observations were acquired by various groups using the International Ultraviolet Explorer Satellite between 1978 and November 1992 ('1'able 1). We analyze this entire data set, including the observations of Butterworth and Meadows, to provide a uniform reduction of all 45 objects.

Wc examine the IUE data to see if taxonomics based on visible and infrared data persist into the ultraviolet. Classification systems arc a first-order means of organizing observations. '] 'axonomic classes of asteroids tend to bc based on color photometry, 0.3- 1.1 μm (summarized by Tholen and Barucci 1989), and radiometry (e.g., Tedesco *et al.* 1992). The original classes (S, C, M, etc.) were based on assumed connections with meteoritic types (S=stony, C= carbonaceous, M=metallic; see Chapman 1979 for a review), although the original and current classification schemes arc based on the observational data rather than composition. A number of schemes currently co-exist, each with strengths and weaknesses, but they arc more descriptive than analytic. Ultraviolet studies should provide additional insight into these properties, particularly with regard to those asteroids that arc difficult to classify.

2. Observations

All low-resolution (4-6 Å) spectra acquired with the IUE satellite between 1978 and November 1992 were obtained from the National Space Science Data Center (NSSDC) archives through the IUE Data Analysis Center, in reprocessed form. Spectra from the large aperture (20 x 9 arcsec) of the Long Wavelength (1900-3300 Å) Primary and Redundant (1 .WP, LWR) cameras were selected. Data from the small aperture or Short Wavelength Primary (SWP) camera did not contain sufficient useful information for this study. The observations arc listed in Table 1.

The quality of the data varies greatly, as shown in Fig. 1. The IUE has a limited dynamic range; long exposures taken to obtain good quality data at shorter wavelengths (lower flux) may bc saturated around 2900 Å. To obtain the best spectrum for each asteroid, wc co-added multiple observations of the same object. When combining spectra, wc eliminated saturated or bad data points and weighted the sums by the inverse square of the deviations. The composite spectra therefore represent the best data available at each wavelength.

2.1 Solar Spec rum

In the Uv, steroids shine by reflected sunlight. The solar flux depends strongly on wavelength in this spectral range. Spectra have low signal (and thus low signal-to-noise ratio) below about 2600 Å because there is relatively little solar continuum to reflect. Longward of 2900 Å, the solar continuum increases, but the sensitivity of the IUE falls, and so the SNR declines. Convolving the. solar continuum with the IUE response functions gives an effective

sensitivity (Fig. 2, top). Around 2670 Å, both the sensitivity and the solar continuum are reasonably high and fairly stable, so we use this region for normalizing the asteroid and solar spectra.

The two center cells of Fig. 2 show an asteroid spectrum (diamonds) with the matched solar continuum (solid line), and the normalized spectral reflectance of the asteroid (asteroid spectrum/normalized solar continuum). The choice of solar spectrum strongly affects the derived asteroid spectrum. We use the solar spectrum acquired by Vanhoosier *et al.* (1988) with the Solar Ultraviolet Spectral Irradiance Monitor (SUSIM) experiment aboard Spacelab 2. This spectrum (henceforth, "SUSIM") seems to fit the continuum of IUE spectra of comets quite well (Budzien 1992), and has a relatively low uncertainty (3.9%). Other possible solar models include the solar analog composite spectrum of A'Hearn (private communication), which was acquired with the same instrument as the asteroid data; the solar spectrum acquired by Mount and Rottman (1981) with a rocket-borne spectrometer; and the solar spectrum published by Broadfoot (1972). The last solar spectrum was used by Butterworth and Meadows. The last two solar spectra do not cover the entire wavelength range needed, but end around 3150 Å. Broadfoot's spectrum has uncertainties as high as 30%.

The variability of Fraunhoffer lines in the Sun's spectrum is one cause of the difference in spectra; they were acquired at different points in the solar cycle. Variation of the solar continuum is minimal in our region of study (4-7%, according to Lean 1987), although the individual line variations can be substantially larger, such as the Mg II doublet near 2800 Å (variation up to ~20%). Because we expect continuum reflection, possible with broad (100 Å or more) absorption bands, and do not expect resonance with the Fraunhoffer lines, we treat the solar continuum as constant in time. We do, however, avoid highly variable wavelength regions when calculating geometric albedos.

The four solar spectra differ by 5-20% (rms) in the range 2200-3100 Å when matched to each other at 2670 Å. IUE pointing drift can affect the wavelengths and change the spectral width of features in the asteroid spectra; small mismatches between the IUE spectra and the solar spectrum can result in spurious features, particularly where the solar continuum is changing rapidly. We set a conservative estimate of the uncertainty due to the shape of the solar spectrum at 20%. Apparent features comparable to or smaller than 20% over a short (<40 Å) wavelength range are thus not reliable.

The lowest cell in Fig. 2 shows the effect of systematic error in the background subtraction. Small errors are magnified at shorter wavelengths when the asteroid spectrum is divided by the solar continuum. The apparent shape of the relative reflectance is affected at shorter wavelengths, but relatively unaffected at longer wavelengths. Apparent features below about 2900 Å are particularly suspect.

3. Analysis

Many of the best relative spectra lack a reliable absolute calibration because the spacecraft pointing accuracy tended to be worst for early observations and long exposures. objects may have drifted out of the aperture to invalidate the exposure time. We therefore evaluate the relative spectral reflectances separately from the absolute geometric albedos.

Our proccdurc for data reduction involved the following steps:

1. Spatially resolved spectra, corrected for geometric distortion and translatable into photometric units using a recent calibration at the Goddard Space Flight Center, were obtained from the NSSDC archives.

2. Spatially resolved spectra were integrated to produce a series of single spectra using standard IUE data reduction programs. Pointing jitter or drifts often kept the source from appearing pointlike, so the spectra were processed as if from an extended source (30 pseudo-orders). Spectral elements containing problematic data (saturated, rescaux marks, etc., as determined by the IUE processing) were flagged.

3. For each exposure, the background was estimated by adding ten unexposed lines along each side of the spectrum. The background spectrum was averaged, filtered, and subtracted from the data. The scaled rms variation of the background was used as an estimate of its uncertaint y.

4. Each spectrum was interpolated to a common1-Å scale; wc also interpolated and scaled the uncertainties. Spectral elements interpol ated from flagged spectral elements were eliminated. The resulting spectra were used to calculate both the net relative spectra and the net absolute spectra.

5. A net relative spectrum for each asteroid was constructed by normalizing available spectra at 2660-2680 Å and co-adding data (section 3.1) before dividing by a solar spectrum matched to the same wavelength range.

6. A net absolute spectrum for each asteroid was constructed by correcting for solar phase angle and observing geometry, and co-adding data (section 3.2). Geometric albedos were determined from these absolute spectra.

3.1 Spectral Reflectance

A net reflectance spectrum for each asteroid was constructed by normalizing individual spectra and co-adding the results (step 5). Each spectrum was normalized at 2660-2680 Å because this range is generally flat, with average signal-to-noise approximately twice the SNR as the normalization point chosen by Butterworth and Meadows (3170 Å). The IUE has a short dynamic range, and this choice also ensured that very fcw spectra were eliminated by lack of good data at the normalization wavelengths. This procedure removes the overall brightness variation duc to illumination and observation distances (Sun-asteroid and asteroid-Iiarth distances), rotational phase variation, and errors in calculated flux duc to the asteroid drifting out of the aperture during an exposure. The spectra were weighted by the inverse-square of their uncertainties, element by element.

Following Butterworth and Meadows (1985) and Festou *et al.* (1991), wc have chosen to add the data spectrally into 20 Å intervals to reduce problems duc to small wavelength or resolution mismatches between the data and the solar spectrum. The solar spectrum was matched to the data at 2670 Å and divided out, leaving a normalized reflectance. (Wavelength-independent reflection would produce a ratio of 1.0.) The results arc presented in Fig. 3. Wc note that data near steep changes in the solar spectrum remain less reliable than those where the solar spectrum is relatively flat. Elements with uncertainties greater than 30%1 arc not plotted, As was demonstrated in Fig. 2, small features (20-40 Å wide) appear to bc artifacts duc to the choice of or division by the solar spectrum. The apparently increasing reflectivity at short wavelengths may be a magnification of small errors in the calibration, background subtraction, and division by relatively low solar flux. Wc cannot say this upturn represents a physical characteristic of asteroids. observations with the 1 Iubble Space Telescope will bc able to clarify (his point.

Spectra of a comet and the Moon, reduced in the same way, arc plotted for comparison. Cometary spectra have emission bands in the UV, and arc more typically shown with the solar continuum subtracted rather than divided. Onc of the emission bands occurs in the 20 Å spectral element used for normalization, so the, baseline of the cometary spectrum is lower than 1.(). Strong emission bands were clipped and arc marked with upward arrows. The lunar

spectrum is shown as a comparison of a body with mineralogical assemblages expected to be similar to S-type asteroids.

As a first-order analysis to identify any spectral differences among the major classes of asteroids, wc compare average spectra for types S, C, and M. Net spectra of objects of type S (asteroids 3,6,7,9, 14, 15, 18,20,23,27,29,40,42, 63,89,433,471, and 532) were co-added, as were asteroids of type C (10, 41, 54, 88, 324,410, and 511) and those of type M (16, 22, 129, and 135).

The net S-type UV spectrum is redder than the net C-type or M-type spectrum (Fig. 4). These results arc consistent with the hypothesis that classes based on the visible and infrared data persist in ultraviolet spectra. Specifically, tbc broad silicate absorption band seen in S-typc asteroids continues into the ultraviolet region of tbc spectrum. The low, flat spectrum of C-type asteroids also continues into the ultraviolet, despite an apparent downturn in the near UV of ground-based spectra (see summary, Tholen and Barucci 1989). "1'here arc no color difference between C-types and M-types within the uncertainty of our data. (See below for discussion of albedo differences.)

3.2 **Geometric Albedo**

The geometric albedo is defined as the flux from a fully illuminated object (solar phase angle of zero) divided by the flux from a perfectly diffusing disk of an equivalent cross-sectional area in the same position. It is a measure of the intrinsic reflectivity of an object, giving information on the composition and basic nature of the surface.

Geometric albedos (p) were calculated from individual absolute spectra (step 6) with the following formula:

$$p = \frac{R^2 \Delta^2}{r^2 \rho^2} \frac{F}{F_S} f(\phi)$$

where R is the Sun-asteroid distance (AU); A is the liarlh-asteroid distance (AU); r is the asteroid radius (km); p is the Sun-Earth distance (= 1 AU); F is the integral flux from the asteroid (erg $s^{-1} cm^{-2} Å^{-1}$); F_S is the flux from the Sun at the Earth in the same units; and $f(\phi)$ is the phase correction (unitless) as a function of Sun-asteroid-F,arth angle (= solar phase angle., ϕ).

The average brightness in four wavelength regions (60 Å wide, centered at 2450,2670, 2950, and 3150 Å) was calculated for each individual spectrum, and divided by the solar flux at 1 AU measured at that wavelength (6.12, 26.8,56.4, and 75.6 erg S-1 cm^{-2} $Å^{-1}$, respectively). The choice of wavelength regions is a compromise between minimizing the solar variability (temporal and spectral) and maximizing the. SNR.

Each brightness was adjusted for Sun-as[croid-ob.server distances, as well as asteroid diameter (from Tedesco *et al.* 1992, except for objects 9, 14,27, 129,433, 1566, and 4015). The diameters given in the literature arc often dependent on class and albedo determination.s, but tend to be consistent with those determined by occultation events (summary, Minis and Dunham 1989) and other techniques (e.g., Drummond and Hege 1989).

Many asteroids, particularly the smaller ones, arc not spherical. For most of the IUE observations, the exposure time is shorter than the lightcurve or rotational period. An observation made when the asteroid is end-on or at the minimum of the lightcurve can give a different result from an observation of the asteroids' largest cross-section or brightness. Longer or multiple exposures will tend to minimize this effect. The range of exposure times and the rotational periods arc listed in I'able 11, as arc the number of exposures contributing to each albedo calculation. Albedos based on single or short exposures should be considered significantly less reliable than those based on long exposures or many exposures. While orbital phase curves have been determined for many of the.sc objects, the uncertainties in the period become unacceptably large when the light curve is extrapolated to the epoch of observation.

~'base curve and correction, To obtain a geometric albedo, it is necessary to extrapolate the measured brightness to a solar phase angle of zero degrees. Several asteroids were observed at multiple phase angles. The brightnesses (corrected for everything except solar phase angle or rotational phase) arc shown in Fig. 5 as a function of phase angle. Where multiple spectra of an object were available within a small range of solar phase angle (-50), the brightest was selected. This selection criterion eliminates exposures where the pointing was very poor, and it tends to select exposures from the peaks of the rotational phase curves. This procedure and the resulting phase curve should be regarded as primitive. Within this framework, these first ultraviolet phase curves of asteroids resemble visible phase curves.

Wc used composite Hapke parameters from Helfenstein and Veverka (1989) to correct for the solar phase effects for C-type and S-type asteroids. For other classes, wc assumed a Henyey Greenstein asymmetry factor of -().35, an opposition surge similar to the composite S-type, and single scattering albedos as follows: E ().50; F 0.06; G 0.09; M 0.15; R 0.40. The phase concoctions range from a factor of 1.02 to a factor of 15 for a solar phase angle of 90°.

For each asteroid, spectra with albedos less than 2% of the maximum were eliminated; the low flux is evidence that the object drifted out of the aperture during exposure. Weighted averages for each asteroid were calculated from the remaining geometric albedos at each wavelength, and arc shown in I'able 11.

Physically unrealistic albedos for objects 1566,2,201, and 4015 arc probably a result of uncertainties in the determination of these diameters. in fact, our technique for determining geometric al bedos identifies asteroids that may have inaccurately determined sizes.

4. **Discussion and Conclusions**

Figure 4 shows that in general, S-type asteroids arc redder than the M- and C-classes. Figure 6 is a color-albedo plot of the three classes (S, C, and M) containing multiple objects. For color, wc usc the ratio of albedo at 3150 Å and that at 2950 Å (60 Å bands), and for albedo wc usc the geometric albedo at 2670 Å. Asteroids classed as C cluster toward the left, M's tend to lie toward the right, and S's tend to lie in the center. (Asteroid numbers identify outliers and specifically discussed objects.) Our work thus shows that the three major asteroid taxonomic classes persist, in a general way, in the ultraviolet region of the spectrum.

The M-types asteroids have UV albedos similar to or exceeding those of S-type asteroids, which is the reverse of the trend in the visible. The spectral albedo of S-type asteroids decreases sharp] y from the visible into the near-LJV, due to the broad absorption band characteristic of siliceous materials (Wagner *et al.*1987), while the M-type albedos remain fairly flat. The low UV albedos of S-type asteroids relative to h4-types show that this absorption band continues below 3500 Å.

As in the visible, the UV albedos of C-types arc notably lower than those of M- and S-type asteroids. Unlike Butterworth and Meadows, wc do not see the albedos of 20 Massalia or 29 Amphitrite as unusual for S-class asteroids. Our calculated UV albedos arc lower than albedos in the visible and near-[JV: -0.02,-0.05, and -0.08 for C, S, and M at 2950 Å, compared to -0.04,-0.10, and -0.12 at 3400 Å (Tedesco *et al.*1989). These albedos can provide a basis for ultraviolet observations with other instruments, such as the Hubble Space Telescope, for which an accurate determination of exposure times will enable efficient usc of spacecraft observing time.

The E-type asteroid 44 Nysa has a much higher UV albedo than other asteroids, 0.273 at 2670 Å, a result that is consistent with its high visual albedo. This object was interpreted to be an iron-free achondritic enstatite, as in aubrite meteorites (Zellner 197S). The UV spectral albedo of 44 Nysa wc observed does show the type. of absorption band displayed by aubrite

(Wagner *et al.* 1987). This UV drop in albedo is sharper for 44 Nysa than for most of the M-type asteroids.

Even though the G-, 1-, and F-type asteroids have higher albedos than C-types in the visible (Tedesco *et al.* 1989), the single examples of these classes in our data set (objects 1, 308, and 704) have UV albedos that are similar to the UV albedos of C-type asteroids.

Butterworth and Meadows did not correct for solar phase angle in their 1985 analysis, arguing that the observations were made within a few degrees of opposition. We found that the corrections to absolute flux (and hence albedo) due to solar phase angle exceed a factor of two for phase angles greater than about 25°. The phase corrections allow us to include some early spectra which were not used by Butterworth and Meadows. Our calculated phase corrections exceed a factor of two for 13 of their 88 spectra, and a factor of 1.5 for 14 more.

For those 10 asteroids with sufficient coverage in solar phase angle, we produced the first UV solar phase curves for asteroids (Fig. 5). The phase curve for 16 Psyche has a steep slope at small phase angle, similar to the well-known non-linear surge in brightness exhibited by most airless bodies at small solar phase angles (< 6°, see Veverka 1977). Data from several additional spectra (not plotted) confirm the brightness at phase angles of 3-4°, but there is only one spectrum at a phase angle near 70, so this should be regarded as an unconfirmed detection of an opposition effect at ultraviolet wavelengths.

Some small bodies have characteristics of both asteroids and comets. Asteroid 4015(1979 VA) was identified as Comet Wilson-1 Barrington 194911 by Bowell (1992). Some of the spectra used here were acquired in searches for cometary emission features (McFadden *et al.* 1993, Schultz *et al.* 1993, and A'Hearn and Feldman 1992). Data acquired by A'Hearn and Feldman include two spectra which were intentionally centered off the nucleus of 1 Ceres (LWP 17155 and LWP 20468). The first shows some reflected solar continuum and was used to calculate the relative, but not absolute, spectrum. The second was saturated and not used, but is listed in Table I for completeness. The spectra presented in Fig. 3 were processed to search for broad absorption bands rather than narrow emission features. We therefore do not expect to see cometary emission features in Fig. 3 unless they are strong compared to the continuum.

As we showed in Section 2.1, small misregistrations between the solar spectrum and the IUE spectrum may result in spurious features. Thus, we must not overly interpret features such as those at 3180 Å and 3075 Å. Some of the spectral features tentatively identified by Butterworth and Meadows, such as those at 2425 Å for 1 Ceres, 4 Vesta, and 44 Nysa, may be artifacts of the process of removing the solar spectrum. These features should receive close scrutiny by the HST, which includes instruments such as the Faint Object Spectrograph that can obtain spectra of much higher signal to noise. Another spectral region which requires

detailed study is that shortward of 2600 Å; this region contains many spectral features of primitive organic materials, including polycyclic aromatic hydrocarbons (Lee and Wdowiak 1993). Our observations suggest an upturn in many of the asteroid spectra in this region, similar to that exhibited by primitive organic materials. Because the signal is small compared to the background, however, an apparent slope can result from a small error in the background subtraction (Fig. 2). Thus, this upturn should not be considered a detection of organic material. It is important to note that for those asteroids with the best (i.e., highest signal to noise) spectra, important differences do appear to occur below 2600 Å (e.g., 1 Ceres and 4 Vesta). The characteristics of this region may prove to be a way to identify those asteroids covered with dark primitive material and those asteroids that have been reprocessed.

Acknowledgments

We are grateful to Dr. C. Imhoff, and to Mr. R. Thompson for assistance with the processing of IUE data. We thank Dr. M. Chahine for his support.

This research was performed at the Jet Propulsion Laboratory, California Institute of Technology, under contract to the National Aeronautics and Space Administration. The work was funded by the NASA Astrophysics Data Analysis Program and the JPL Postdoctoral Program. The IUE spectra were obtained through the IUE Working Group from the National Space Science Data Center Archives.

References

A'] learn, M. F., and P. D. Feldman 1992. Water vaporization on Ceres. *Icarus* 98,54-60.

Binzel, R.P. and S. Xu 1993. Chips off of asteroid 4 Vesta: Evidence for the parent body of basaltic achondrite meteorites. *Science* 260, 186-191.

Bowel], E. 1992. *IAU Circular* 5585.

Broadfoot, A.I,., 1972. The solar spectrum 2100-3200 Å. *Astrophys. J.* 173,6$1-689.

Budzien, S. A., 1992. *Physical and Chemical Processes of the Inner Coma Observed in Mid-Ultraviolet Cometary Spectra.* PhD dissertation, Johns Hopkins Univ., Baltimore.

Butterworth, P. S., and A.J. Meadows, 1985. Ultraviolet reflectance properties of asteroids. *Icarus* 62,305-318:

Butterworth, P. S., A.J. Meadows, G. E. Hunt, V. Moore and D. M. Willis 1980. Ultraviolet spectra of asteroids. *Nature 287, 701-702.*

Chapman, C. R., 1979. The asteroids: Nature, interrelations, origin, and evolution. in *Asteroids (T.* Gehrels, Ed.), pp. 25-60. The Univ. of Arizona Press, Tucson.

Drummond, J. D. and E. K. Hege 19$9. Speckle interferometry of asteroids. In *Asteroids II* (R.P. Binzel, T. Gehrels and M.S. Mathews, Eds.) pp. 171-191. The Univ. of Arizona Press, Tucson.

Festou, M. C., S.A. Stern and G.P. Tozzi 1991. Asteroid 4 Vesta: Simultaneous visible and ultraviolet IUE Observations. *Icarus* 94, 218-231.

Helfenstein, P., and J. Veverka 1989. Physical characterization of asteroid surfaces from photometric analysis. In *Asteroids II* (R.P. Binzel, T. Gehrels and M.S. Mathews, Eds). pp. 557-593. The Univ. of Arizona Press, Tucson.

Lagerkvist, C. 1., A. Harris and V. Zappala 1989. Asteroid lightcurve parameters. In *Asteroids II* (R.P. Binzel, 'T'. Gehrels and M.S. Mathews, Eds.) pp. 1162-11 "?9. The Univ. of Arizona Press, Tucson.

Lean, J. 1987. Solar ultraviolet irradiance variations: A review. *J. Geophys. Research* 92,839-868.

Lee, W. and T.J. Wdowiak 1993. Laboratory spectra of polycyclic aromatic hydrocarbon ions and the interstellar extinction curve. *Astrophys. J. 410,* 1.127-1.130.

McFadden, I.,. A., A.L Cochran, E.S. Darker, D.P. Cruikshank, and W.K. Hartmann 1993. The enigmatic object 2201 Oljato: Is it an asteroid or an evolved comet? *J. Geophys. Research* 98,3031-3041.

Minis, R .1.. and D. W. Dunham 1989. Precise measurement of asteroid size and shapes from occultations. In *Asteroids II* (R.P. Binzel, T. Gehrels and M.S. Mathews, Eds), pp. 148-170. The Univ. of Arizona Press, Tucson.

Mount, G. H. and G.J. Rottman 1981. The solar spectral irradiance 1200-3184 near solar maximum: July 1 S, 1980.1. *Geophys. Research* 886, 9193-9198.

Shultz, R., M.F. A'Hearn, LA. McFadden, D.K. Yeomans, M.E. Haken, and A. Chamberlin 1993.2201 Oljato and 1566 Icarus: Comets or asteroids? A comparison with Comet Wilson-Barrington also known as Asteroid (4015) 1979 VA, In IA *U Symposium 160: Asteroids, Comets, Meteors 1993* (Abstracts), p. 264.

Stern, S. A., M.C. Festou, J. Van Santvoort, and B.J. Buratti 1990. The first UV spectrum of a uranian satellite: IUE Observations of Oberon. *Astron. J. 100, 1676-11679.*

Tedesco, E.F., G. J. Veeder, J. W. Fowler and J.R. Chillemi 1992. *The IRAS Minor Planet Survey*. Phillips Laboratory, Hanscom Air Force Base, MA.

Tedesco, E.F. J. G. Williams, D. L. Matson, and G.J. Veeder, 1989. A three-parameter asteroid taxonomy. *Astron. J. 97, 580-606.*

Tholen, D.J. 1989. Asteroid taxonomic classifications. in *Asteroids II* (R.P. Binzel, T. Gehrels and M.S. Mathews, Eds.), pp. 1139-1150. The Univ. of Arizona Press, Tucson.

Tholen, D.J. and M.A. Barucci 1989. Asteroid taxonomy. In *Asteroids II* (R.P. Binzel, T. Gehrels and M.S. Mathews, Eds.), pp. 298-315. The Univ. of Arizona Press, Tucson.

Vanhoosier, M.E., J.F. Bartoe, G.E. Brueckner and D.K. Prinz 1988. Absolute solar spectral irradiance 120 nm -400 nm (Results from the solar ultraviolet spectral irradiance monitor-SUSIM-experiment on board Spacelab 2). *Astro. Lett and Communications* 27, 163-168.

Veverka, J. 1977. Photometry of satellite surfaces. In *Planetary Satellites* (J.A. Burns, Ed.), pp.17 1-209. The Univ. of Arizona Press, Tucson.

Wagner, J. K., B.W. Hapke, and E.N. Wells 1987. Atlas of reflectance spectra of terrestrial, lunar, and meteoritic powders and frosts from 92 (o 1800 nm. *Icarus* 69, 14-28.

Weissman, P.R., M.F. A'Hearn, L.A. McFadden and H. Rick man 1989. Evolution of comets into asteroids. In *Asteroids II* (R.P. Binzel, T. Gehrels and M.S. Mathews, Eds.), pp. 880-920. The Univ. of Arizona Press, Tucson.

Zellner, B. 1975.44 Nysa: An iron-depleted asteroid. *Astron. J.* 198, L45-L47.

'l'able I: **Observations**

Image	Year	Day	Time (tJ'J')	Exposure duration (s)	Phase angle (deg.)	Distance from sUn (AU)	Program Earth (AU)	ID	Observer(s) (from image headers)
1 ccl-t's									
LWR 1890	1978	206	08:15	1200	6.7	2.92	1.94	PSMGT	Tomasko
LWR 5688	1979	268	00:34	521	6.7	2.93	1.96	SABDM	Matson, Nelson
LWR 5689	1979	268	01:09	3600	6.7	2..93	1,96	SABDM	Matson
LWR 6107	1979	316	19:21	1260	14.2	2.90	2.12	UK228	Butterworth
LWR 9501	1980	350	09:15	300	11.6	2.61	1.73	SACDM	Nelson, Veeder
LWR 16197	1983	172	14:18	1200	17.0	2.96	2.30	SPERN	Nelson, Tedesco
LWR 16198	1983	17'2	15:42	1620	17,0	2.96	2.30	SPERN	Nelson, Tedesco
LWP 17155	1990	14	16:02	33000	1.2	2.64	1.75	OD69Y	A'Hearn, Feldman <1>
LWP 17156	1990	15	02:06	1200	1.3	2.64	1.75	OD69Y	A'Hearn, Feldman
LWP 171s7	1990	15	03:32	300	1.4	2.64	1.75	0D69%	A'Hearn, Feldman
LWP 20468	1991	149	08:15	27000	6.4	2.66	1.87	SCMMA	A'Hearn, Feldman <1>
LWP 20469	1991	149	16:52	360	6.S	2.66	1.88	SCMMA	A'Hearn, Feldman
LWP 20470	1991	149	17:34	1800	6.S	2.66	1.88	SCMMA	A'Hearn
LWP 23407	1992	182	06:02	26400	10.2	2.94	2.02	COOMA	McFadden, Hakes
LWP 23408	1992	182	13:59	420	10.1	2.94	2.02	COOMA	McFadden, Hakes
LWP 2,3783	1992	240	02:53	21600	12.2	2,96	2.10	COOMA	A'Hearn, Haken
2 **Pallas**									
LWR 1540	1978	142	15:06	600	14.5	3.08	2.33	PSMGT	Zellner
LWR 5370	1979	229	04:00	6000	7.8	3.39	2.4S	SABDM	Nelson
LWR 5371	1979	229	06:17	3000	7.8	3.39	2.45	SABDM	Nelson
LWR 5372	1979	229	07:36	2400	7.8	3.39	2.4S	SABDM	Nelson
LWR 5373	1979	229	08:41	2400	7.8	3.39	2.45	SABDM	Nelson
LWR 9493	1980	349	18:30	1200	22.0	2.50	2.01	SACDM	Veeder, Nelson, McCord
LWR 9494	1980	349	19:22	1200	22.0	2.50	2,01	SACDM	Veeder, Nelson, McCord
3 Juno									
LWR 1896	1978	207	08:36	3600	5.5	2,81	1.82	PSMGT	Tomasko, Zellner
LWR 5678	1979	267	04:02	2160	29.5	2.00	1.93	SABDM	Matson
LWR 5679	1979	267	05:09	4860	29.5	2.00	1.93	SABDM	Matson
LWR 5690	1979	268	03:24	9900	29.6	2.00	1.92	SABDM	Matson, Nelson
LWR 6487	979	363	05:05	2880	2.7	2.14	1,22	SPBMT	Zellner
4 **Vesta**									
LWR 2201	978	240	22:23	900	7.3	?.17	1.76	UK043	Butterworth
LWR 5676	979	267	00:37	420	7.6	2.51	1.73	SABDM	Matson
LWR S677	979	267	01:21	4200	7.6	2.51	1.73	SABDM	Matson
LWR 6106	979	316	17:05	600	S.8	?..54	1.s7	UK228	Butterworth
LWR 10S84	1981	132	15:58	1680	25.8	2.30	1.93	SADDM	Matson, Lane
LWR 10610	1981	134	12:37	1200	25.9	2..30	1.9s	SADDM	].ant, Veeder, Matson
LWR 10611	1981	134	14:11	1200	25.9	2.30	1.95	SADDM	I.ant, Veeder, Matson
LWR 13163	1982	124	15:40	500	27.5	2.18	1.97	SAEDM	Lane
LWP 5589	1985	82	18:03	80	14.4	2.?2	1.32	SPGRN	Nelson, Lane
LWP 5590	985	82	18:40	150	14.4	2.22	.32	SPGRN	Nelson, Lane
LWP 5602	985	84	01:55	135	13.9	2.22	.31	SPGRN	I.ant, Nelson
LWP 1622.9	989	240	06:20	140	24.6	2.19	.s7	SNLRW	Wagener
LWP 18949	990	279	15:18	300	17.1	2.54	.76	MSTOO	Tozzi (Festou?)
LWP 18950	990	279	16:01	300	17.1	2.54	.76	MS-I'(X)	Tozzi
LWP 18951	990	279	16:46	300	17.1	2.54	.76	MSTOO	Tozzi
LWP 18952	1990	279	17:32	300	17.1	2.54	1.76	MSTOO	Tozzi
LWP 189S3	1990	279	18:14	300	17.1	2.54	1.76	MSTOO	Tozzi

Table 1: Observations

Image	Year	Day	Time (UT)	Exposure duration (s)	Phase angle (deg.)	Distance from Sun (AU)	Distance from Earth (AU)	Program ID	Observer(s) (from image headers)
LWP 18954	1990	279	18:59	330	17.1	2,54	1.76	MS1OO	Tozzi
LWP 18955	1990	279	19:40	330	17.0	2.54	1.76	MSTOO	Tozzi
LWP 189S6	1990	279	20:32	300	17.0	2.54	1.76	MSTOO	Tozzi
LWP 18957	1990	279	21:28	330	17.0	2.54	1.76	MAO17	Festou
LWP 18958	1990	279	22:17	390	17.0	2.54	1.76	MAO17	Festou
LWP 18959	1990	279	23:07	390	17.0	2.54	1.76	MAO17	Festou
LWP 18960	1990	279	23:59	390	17.0	2.S4	1.76	MAO17	Festou
LWP 18961	1990	280	00:47	390	17,0	2.54	1.76	MAO17	Festou
LWP 18962	1990	280	01:34	390	17.0	2.54	1.76	MAO17	Festou
LWP 18963	1990	280	02:24	390	17.0	2.54	1.76	MAO17	Festou
LWP 18964	1990	280	03:12	390	17.0	2.54	1.76	MAO17	Festou
LWP 18965	1990	280	03:59	1500	16.9	2.54	1.76	MAO] 7	Festou
6 Hebe									
LWR 9488	1980	348	08:20	3000	19.1	2?.04	1.20	SACDM	Nelson, Veeder
LWR 9495	1980	349	20:36	1800	19.2	2.04	1.21	SACDM	Veeder, Nelson, McCord
LWR 9496	1980	349	21:36	1500	19.2.	2.04	1.21	SACDM	Veeder, Nelson, McCord
LWR 9979	1981	53	11:33	7440	27.0	2.18	2.00	UK359	Butterworth
7 Iris									
LWR 9486	1980	348	05:30	1140	31.7	1.85	1.40	SACDM	Nelson, Veeder
LWR 9487	1980	348	06:22	3000	31.7	1,85	1.40	SACDM	Nelson, Veeder
8 Flora									
LWR 7901	1980	151	15:47	5400	3.1	2.46	1.45	SACDM	Nelson, Veeder
LWR 7902	1980	151	19:13	3720	3.1	2.46	1.45	SACDM	Nelson, Veeder
9 Metis									
LWR 1895	1978	207	05:16	3000	11.1	2.48	1.53	PSMGT	Tomasko
LWR 10880	1981	168	11:58	4500	6.7	2.68	1.69	SADDM	I .ane, Nelson
LWR 10893	1981	169	12:19	5160	7.1	2.68	1.70	SADDM	I.ant, Nelson
10 Hygiea									
LWR 1891	1978	206	10:00	4800	13.8	2..81	1.97	PSMGT	Tomasko, Zellner
LWR 9497	1980	349	23:07	8220	8.0	3.51	2.62	SACDM	Veeder, Nelson, McCord
LWR 9498	1980	350	02:10	7200	8.0	3.51	2.62.	SACDM	Veeder, Nelson
14 Irene									
LWR 7883	1980	149	22:55	2100	9.4	2.29	1.32.	SACDM	Veeder, Nelson
LWR 7900	1980	151	13:14	3600	10.0	2.30	1.33	SACDM	Nelson, Veeder
15 Eunomia									
LWR 7903	1980	151	22:23	3900	13.9	2.77	1.92	SACDM	Nelson, Veeder
16 Psyche									
LWR 1538	1978	142	09:28	4500	4,7	3.24	2.2s	PSMGT	Zellner
LWR 5362	1979	228	04:29	13800	4.2	2.71	1.71	SABDM	Nelson
LWR 9481	1980	347	19:39	4500	3.1	2.68	1.71	SACDM	Nelson, Vccdcr, McCord
LWR 9482	1980	347	21:38	3300	3.1	2.68	1.71	SACDM	Nelson, Veeder, McCord
LWR 9483	1980	347	23:29	1800	3.2	2.68	1.71	SACDM	Nelson, Vccdcr, McCord
LWR 9557	1980	357	11:15	2400	7.0	2.70	1.75	UK359	Butterworth
LWR 12.299	1982	7	03:47	8040	15.9	3.17	2.59	SADDM	Nelson, Ockert
18 Melpomene									
LWP 3671	1984	180	17:41	4200	13.8	?.46	1.ss	SPGRN	Nelson
LWP 3675	1984	181	09:42	4500	14.1	2.45	1.56	SPGRN	Ne lson
20 Massalia									

Table I: observations

Image	Year	Day	Time (UT)	Exposure duration (s)	Phase angle (deg.)	Distance from Sun (AU)	Distance from Earth (AU)	Program ID	observer(s) (from image headers)
IWR 10598	1981	133	14:50	6300	25.2	2.30	1.84	SADDM	Lane, Matson, Veeder
IWR 10612	1981	134	15:29	5400	25.2	2.30	1.85	SADDM	Lane, Veeder, Matson
21 **Lutetia**									
IWR 12301	1982	7	16:49	11520	26.1	2.23	2.09	SADDM	Nelson, Ockert
22 **Kalliope**									
IWR **12303**	**1982**	8	00:40	8100	15.9	2.63	1.87	SADDM	Nelson, Ockert
23 Thalia									
IWR **9499**	**1980**	350	06:04	3000	4.5	2.11	1.14	SACDM	Veeder, Nelson
IWR **9500**	**1980**	350	07:27	2400	4.5	2.11	1.14	SACDM	Veeder, Nelson
27 Euterpe									
IWR 6484	1979	362	19:03	3000	8.5	1.94	0.98	SPBMT	Zellner
29 **Amphitrite**									
IWR 10865	1981	166	12:28	3120	11,2	2.74	1.82	SADDM	Lant, Nelson
IWR 10866	1981	166	14:06	4200	11.2	2..74	1.82	SADDM	l.ant, Nelson
IWR 10873	1981	167	12:21	4200	11.6	2.74	1.83	SADDM	I.ant, Nelson
40 **Harmonia**									
IWR **12297**	**1982**	6	19:51	9900	20.3	2.35	1.65	SADDM	Nelson, Ockert
41 Daphne									
IWR 11366	1981	230	19:53	20520	9.8	2.54	1.59	UK420	Butterworth
IWP 5829	1985	115	23:32	3000	14.7	2.04	1.11	SPGRN	Nelson, Tedesco
42 **Isis**									
IWR 13751	1982	203	19:13	1500	17.6	1,97	1.06	SAEDM	Veeder
44 **Nysa**									
IWR 1907	1978	209	05:59	7200	14.9	2.76	1.94	PSMGT	Tomasko, Zellner
IWR 1908	1978	209	09:05	7200	15.0	2.76	1.95	PSMGT	Tomasko, Zellner
IWR 9946	1981	49	23:10	5100	13.1	2.17	1.26	SACDM	Lane, Nelson
IWR 9947	1981	50	01:41	3000	13.0	2.17	1.26	SACDM	Lane, Nelson
IWR 9958	1981	50	23:19	3000	13.0	2.17	1.26	SACDM	Nelson, Lane
IWR 9977	1981	53	06:55	2400	12.6	2,17	1.25	UK359	Butterworth
IWR 99-/8	1981	53	08:00	6000	11.4	2.18	1.24	UK359	Butterworth
S1 **Nemausa**									
IWR **9559**	**1980**	357	17:18	900	12.9	2.40	1.51	UK359	Butterworth
IWR **12736**	**1982**	67	00:09	4500	22.4	2.22	1.54	SADDM	Nelson, Veeder
IWR 12755	1982	68	21:25	7200	22.0	?.22	1.52	SADDM	Nelson, Veeder
IWR 12766	1982	70	11:41	9900	21.6	2.22	1.50	SADDM	Nelson
S4 Alexandra									
IWR 127S0	1982	68	13:15	10800	6.5	2.89	1.93	SADDM	Nelson, Veeder
IWR 12759	1982	69	12:01	12900	6.3	2.89	1.93	SADDM	Nelson, Veeder
IWR 16799	1983	259	00:55	9720	13.9	2.2.4	1.33	SPERN	Nel son
63 Ausonia									
IWR 7879	1980	149	09:16	4800	17.6	?.18	1.30	SACDM	Veeder, Nelson
IWR 7880	1980	149	11:20	8000	17.6	2.18	1.30	SACDM	Veeder, Nelson
IWR 7899	1980	151	08:45	11200	18.3	2.17	1.31	SACDM	Nelson, Veeder
88 Thisbe									
IWR 11352	1981	229	00:34	4080	20.9	2.34	1.61	UK420	Butterworth, Eaton
89 Julia									
IWR 1230S	1982	8	06:38	3180	6.9	2.57	1.62	SADDM	Nelson, Ockert

Table 1: Observations

Image	Year	Day	Time (UT)	Exposure duration (s)	Phase angle (deg.)	Distance from Sun (AU)	Distance from Earth (AU)	Program ID	Observer(s) (from image headers)
129 **Antigone**									
LWR 1 13s0	1981	228	19:12	6000	20.8	2.37	1.65	UK420	Butterworth, Eaton
135 Hertha									
LWR 11351	1981	228	22:19	3000	10.6	1.94	**0.96**	UK420	Butterworth, Eaton
216 **Kleopa ra**									
LWR 12296	1982	6	16:55	6300	16.3	2..81	2.11	SADDM	Nelson, Ockert
308 **Polyxo**									
LWR 12730	1982	66	13:06	8100	0.9	2.81	1.82	SADDM	Nelson, Veeder
324 Bamberga									
LWR **13674**	**1982**	**194**	7:52	2400	6.1 '	2.21	1.21	SAEDM	Veeder
LWR 13675	1982	194	9:29	900	6.1	2.21	1.20	SAEDM	Veeder
LWR 13750	1982	203	7:12	2100	5.3	2.17	1.17	SAEDM	Veeder
349 **Dembowska**									
LWR 7878	1980	149	2:59	15000	5.7	3.12	2.14	UK359	Butterworth
LWR 7881	1980	149	14:41	13500	5.9	3.12	2.14	SACDM	Veeder, Nelson
LWR 7882	1980	149	19:23	8280	5.9	3.12	2.14	SACDM	Veeder, Nelson
354 **Eleonora**									
LWR 12298	1982	7	00:04	5700	13.2	2.48	1.61	SADDM	Nelson, Ockert
410 **Chloris**									
LWR 16196	**1983**	**172**	11:12	**4980**	1,6	2.08	1,07	SPERN	Nelson, Tedesco
433 Eros									
LWR **12302**	**1982**	**7**	21:49	**6000**	48.8	1.16	0.31	SADDM	Nelson, Ockert
471 Papagena									
LWR **12304**	**1982**	**8**	04:16	**3900**	12.1	2.40	1.50	SADDM	Nelsou, Ockert
511 Davida									
LWR 6485	1979	362	21:11	14400	16.9	2.64	**1.91**	SPBMT	Zellner
532 **Herculina**									
LWR 12300	1982	7	07:19	1320	10.5	2.47	1.55	SADDM	Nelson, Ockert
LWR 15360	1983	54	21:15	1800	21.7	2.48	2.68	SAEDM	Nelson
654 **Zelinda**									
LWR 9558	1980	357	14:03	4800	6.4	1.88	0.90	UK359	Butterworth
7 0 4 **Interamnia**									
LWR 9484	1980	348	01:20	4500	6.0	2.79	1.83	SACDM	Nelson, Veeder, McCord
LWR 9485	1980	348	03:09	4500	6.1	2.79	1.83	SACDM	Nelson, Veeder, McCord
1566 Icarus									
LWP 21370"	1991	273	00:28	23400	90.0	0.85	0.s4	SCNMA	A'Hearn
2201 **Oljato**									
LWP 24103	1992	288	22:13	25260	53.4	1.19	0.99	COOMA	McFadden
LWP 24140	1992	297	22:01	22980	59.2	1.08	0.91	COOMA	A'Hearn, Haken
LWP 24245	1992	307	20:30	9300	66.0	0.97	0.85	COOMA	McFadden
401S **Wilson-Harrington**									
LWI' 2.4039	1992	274	23:41	22140	60.4	1.13	0.75	COOMA	A'Hearn
24046	1992	275	22:14	22200	60.0	1.14	0.75	COOMA	A'Hearn

Note:

<1> LWP 17155 and 20468 did not have 1 Ceres centered in the aperture. The former shows some reflected solar continuum; the latter is saturated and not used.

Table II: Asteroids and UV albedos

asteroid	class <1>	diameter (km) <3>	exposure time (hr) <4>	rotation period (hr)	albedo, uncertainty, number of contributing spectra <5> — 2400 A	2670 A	2950 A	3150 A
1 Ceres	G	848.4	*0.1-0.4*	9.1	0.025 0.001 10	*0.024 0.001 10*	**0.027** 0.001 8	0.030 0.001 10
2 Pallas	B	498.1	**0.2-1.7**	**7.8**	**0.058 0.002** 7	0.051 **0.001 6**	**0.056 0.001 6**	0.059 0.001 7
3 Juno	s	**233.9**	**0.6-2.8**	**7.2**	**0.056 0.003 5**	0.051 0.002 4	**0.063 0.002** 3	0.067 0.002 4
4 Vesta	V	468.3	0.0-1.2	5.3	**0.065 0.002 28**	0.076 0.001 27	0.0s9 0.002 25	0.102 0.002 27
6 Hebe	s	185.2	0.4-2.1	7.3	0.070 0.004 4	0.066 0.003 4	0.078 0.004 3	0.0S6 0.004 4
7 Iris	s	199. s	0.3-0.s	7.1	0.062 0.005 2	0.062 0.004 2	0.069 0.004 2	0.0s1 0.003 2
8 Flora	s	135.9	1.0-1.5	12.s	0.068 0.006 2	0.052 0.002 2	0.057 0.004 2	0.064 0.002 2
9 Metis	s	179.0	0.8-1.4	5.1	0.049 0.004 3	0.036 0.001 3	0.039 0.002 3	0.048 0.002 3
10 Hygiea	c	407. !	1.3-2.3	1s.4	0.03s 0.002 3	0.028 0.001 3	0.028 0.001 3	0.032 0.001 **3**
14 Irene	s	153.0	0.6-1.0	9.4	0.064 0.006 2	0.052 0.003 2	0.061 0.002 2	0.062 0.004 **2**
! 5 Eunomia	s	255.3	1.1-1.1	6.1	0.065 0.010 1	0.051 0.005 I	0.064 0.005 1	0.075 0.004 1
16 Psyche	M	253.2	0.5-2.2	4.2	0.065 0.003 6	0.063 0.002 6	0.066 0.002 5	0.065 0.002 6
! 8 Melpomene	S	140.6	1.2-1.2	11.6	0.077 0.007. 2	0.076 0.003 2	0.0s0 0.003 2	0.092 0.003 2
20 Massalia	s	145.5	1.5-1.8	S.1	0.11S 0.016 2	0.055 0.003 2	0.075 0.003 2	0.072 0.003 2
2 I Lutetia	M	95. s	3.2-3.2	8.2	0.127 0.019 1	0.097 0.005 I	0.108 0.011 I	0.113 0.006 1
22 Kalliope	M	181.0	2.2-2.2	4.1	0.060 0.010 1	0.064 0.003 !	0.061 0,007 1	0.077 0.004 I
23 Thalia	s	107.5	0.7-0. s	12.3	**0.064 0.007** 2	0.056 0.002 2	0.065 0.002 2	0.068 0.003 **2**
27 Euterpe	s	117.0	0.8-0.8	S.5	**0.059 0.006 I**	0.056 0.006 1	--- --- 0	0.070 0.007 1
29 Amphi trite	S	212.2	0.9-1.2	5.4	**0.076 0.007 3**	0.055 0.002 **3**	**0.061 0.002** 3	0.067 0.002 3
40 Harmonia	S	107.6	2. S-2.8	9.1	0.0s4 0.013 1	0.053 0.003 I	0.05s 0.003 1	0.079 0.004 1
4 ! Daphne	c	174. 0	0. 8-5.7	6.0	0.023 0.002 2	0.016 0.001 **2**	0.019 0.001 2	0.024 0.001 2
42 Isis	s	100.2	0.4-0.4	13.6	0.102 0.023 1	**0.065 0.005 1**	0.065 0.003 I	0.072 0.005 1
44 Nysa	E	70.6	0.7-2.0	6.4	0.279 0.015 7	0.273 **0.00S** 7	0.297 0.009 5	0.33'7 0.01: 7
5 ! Nemausa	CU	147.9	0.2-2.S	7.8	().()47 ().()()5 4	**0.025 0.002 4**	0.029 0.001 4	0.033 0.002 4
54 Alexandra	C	165.8	2.7-3.6	7.0	0.027 0.002 3	0.019 0.001 3	0.022 0.001 3	0.024 0.001 3
63 Ausonia	S	103.1	1.3-3.1	9.3	0.056 0.006 3	0.038 0.001 3	0.042 0.002 3	0.051 0.002 3
88 Thisbe	CF	200.6	1.1-1.1	6.0	0.046 0.009 1	0.026 0.002 1	0.031 0.003 1	0.035 0.002 1
89 Julia	s	151.5	0.9-0.9	11.4	0.059 0.011 1	0.029 0.002 1	0.038 0.003 1	0.036 0.002 1
129 Antigone	M	113.0	.1.7- 1.7	5.0	0.123 0.021 1	0.103 0.006 1	0.114 0.010 1	0.117 0.007 1
135 Hertha	M	79.2	0.8-0.8	S.4	0.0S6 0.012 1	0.064 0.004 1	0.075 0.007 1	0.0s1 0.004 1
2 1 6 Kleopatra	M	135.1	**1. S-1.8**	**5.4**	0.245 0.047 I	0.100 0.007 I	0.108 0.010 1	0.133 0.00s 1
308 Polyxo	T	140.7	2.2-2.2	12.0	0.046 0.008 1	0.023 0.002 i	0.025 0.002 i	0.027 0.002 1
324 Bamberga	CP	229.4	0.2-0.7	29.4	*0.024 0.002* **3**	0.021 0.001 3	**0.023 0.001 2**	0.023 0.001 3

Table II: **Asteroids and UV albedos**

asteroid	class <1>	diameter (km) <3>	exposure time (hr) <4>	rotation period (hr)	albedo, uncertainty, number of contributing spectra <5> 2450 A			2670 A			2950 A			3150 A		
349 Dembowska	R	139.8	2.3..4.2	4.7	0.075	0.007	3	0.053	0.002	3	**0.064**	**0.002**	**3**	0.070	0.002	3
354 Eleonora	s	155.2	1.6-1.6	4.3	0.076	0.011	1	0.042	0.003	1	**0.048**	**0.002**	1	0.058	0.004	I
410 Chloris	c	123.5	*1.4-1.4*	32.5	0.028	0.003	I	0.017	0.001	I	0.022	0.001	1	0.022	0.001	1
433 Eros	s	23.0	*1.7-1.7*	**5.3**	0.097	0.014	1	0.075	0.005	1	0.083	0.004	I	0.091	0.006	1
471 Papagena	S	134.2	*1.1-1.1*	**7.1**	0.046	0.011	1	0.052	0.003	1	0.055	0.003	1	0.055	0.004	1
511 Davida	c	326.1	*4.0-4.0*	**5.1**	0.026	0.008	I	0.021	0.001	1	---	---	0	0.025	0.001	1
532 Herculina	S	222.2	*().4-().5*	9.4	0.052	0.017	2	0.040	0.003	2	0.045	0.002	2	0.050	*0.004*	2
654 Zelinda	C	127.4	1.3-1.3	31.9	0.058	0.010	I	0.045	0.003	1	().()49	0.002	1	**0.048**	0.015	1
704 Interamnia	F	316.6	1.2-1.2	8.7	0.031	0.002	2	0.026	0.002	2	0.028	0.001	**2**	**0.029**	**0.00!**	2
1566 Icarus	S <2	1.0 <6>	6.5-6.5	2.3	3.987	6.821	1	11.004	0,840	1	14.404	0.705	1	**21.160**	**1.505**	I
2201 Oljato	S <2	1.8 <6>	2.6-7.0	24.0	1.905	1.877	2	1.545	0.137	2	2.307	0.118	**2**	**6.535**	**0.342**	2
4015 Wilson-Barrington	CF	3.0 <6>	6.2-6.2	3.6	3.811	2.752	2	1.550	0.268	2	3.035	0.192	**2**	**3.366**	**0.398**	2

Notes:

<1> Asteroid classes are from Tholen 1989. Primary classification (first letter) was used for the phase correction.

<2> **Assumed** to be S-type.

<3> Diameters are from **Tedesco et al.** 1992.

<4> **Range** of exposure times for the contributing IUE spectra; compare to rotation period from Lagerkvist et al. 1989.

<5> Albedo, uncertainty, and number of contributing spectra for the 60-Angstrom band centered at each wavelength.
The following exposures had unreliable exposure times or calibrations, and were **excluded** from the above calculations (see text): 1: LWR 5689, LWP 17155, LWP 20468, LWP 20470. 2: LWR 5370. **4:** LWR 5677. 44: LWR 9947. 2201: LWP 24245.
Several other spectra were saturated and did not contribute to the individual albedo calculations.

<6> Physically unrealistic albedos may be a result of **unusually** small **diameter values.**

Figure Captions

Figure 1: Sample spectra

Examples of high, typical and low signal-to-noise spectra at original resolution. The vertical bars represent the uncertainty at each resolution element. Spectral elements with uncertainties greater than the flux near 2950 Å, as wc]] as those affected by reseaux (fiducial) marks, arc not plotted.

Figure 2: Solar spectrum effects

TOP: Solar continuum as measured from the SUSIM experiment aboard Spacelab 2, convolved with the IUE spectral sensitivity. This approximates the spectral dependence of the signal-to-noise ratio (SNR). The best SNR occurs near 2950 Å, but the solar continuum varies rapidly in this region. A relatively good SNR and a relatively flat solar continuum occur shortward of 2700 Å, and this region was chosen for normalization of the spectra.

CENTER TOP: Spectrum (LWP 3675) of asteroid 18 Melpomene, binned to 20 Å resolution (diamonds). Solar continuum (solid line) was matched to the data at 2660-2680 Å.

CENTER BOTTOM: Effects of different solar continuum models on derived asteroid spectrum. Data was divided by three solar spectra; SUSIM (diamonds), Mount and Rottman 1981 (dotted line), and Broadfoot 1972 (dashed line) as well as a solar analog composite spectrum. This graph shows that many features may be artifacts of the solar model, particularly below 2600 Å, where the solar continuum and IUE sensitivity arc low.

BOTTOM: Effect of systematic error in the IUE background subtraction. The dotted and dashed lines were produced by adding and subtracting 0.4x10- ^{14} erg s^{-1} cm^{-1} Å^{-1} from the data before dividing by the solar model. Small errors in the background subtraction can produce or change spurious features (such as those around 2800 Å and 2600 Å) but they do not produce the overall redness seen in many of the asteroid spectra.

Figure 3: Normalized UV asteroid spectra

Available IUE spectra for each asteroid were matched at 2670 Å and co-added, then divided by a solar model. Dotted lines at 1.0 represent spectrally uniform reflectance. Co-added cometary and lunar spectra, processed in the same manner, arc shown for comparison. The locations of cometary emission bands arc shown. Two spectra of comet Wilson (1987 VII) arc co-added (LWP 10627, LWP 10628) and seven spectra of the Moon arc co-added (LWR 5719, LWR 6091, LWR 6093, LWR 8626, LWR 9970, LWP 13622, and LWP16559). Elements with uncertainties greater than 30% arc not plotted, except for object 4015, where

spectral elements with uncertainties up to 40% are plotted in order to retain the normalization point.

Figure 4: Comparison of S, C, and M-class composites

Spectra of generally uncontested S-class asteroids (3,6,7, 8, 9, 14, 15, 18,20,23,27,29, 40,42, 63, 89,433,471, 532) were co-added to produce a composite S-class UV spectrum. Similar] y, composite spectra were constructed for C-class(1O,41, 54,88,324,410,511) and M-class (16,22, 129, 135) asteroids. Differences in these composites spectra suggest that the classification schemes based on visible and infrared data are applicable to ultraviolet data. The composite M and C spectra show no overall difference (slope 0.7x10-S +/- 2.1x10-5 is equal to zero within error), but the composite S spectrum is redder than the C spectrum (slope 1.4x10-4 +/- 0.2x 10-4 is not equal to zero).

Figure S: UV phase curves

The dependence of brightness on solar phase angle is shown for ten asteroids, labeled by their number. The brightness have been corrected for heliocentric and geocentric distances, and asteroid diameter; they are equal to the geometric albedo if extrapolated to a solar phase angle of O^{o}. The data represent individual spectra; where several spectra were available within a small (typically 5°) range of phase angle, the spectrum with the highest value was chosen. This procedure eliminates exposures with poor pointing and tends to select maxima of the rotational curve. in most cases, however, the unknown rotational geometry leaves a high uncertainty in the brightness.

Figure 6: Color vs albedo

'l-hc ratio of geometric albedos at 3150 Å and 2950 Å (larger values indicate reddened spectra) are plotted as a function of geometric albedo at 2670 Å (where the solar model was matched for the relative reflectance spectra). Errors are comparable to the plotting symbols in the vertical direction, 1-5 times the symbol size in the horizontal direction. Some of the outlying points are labeled with asteroid numbers.

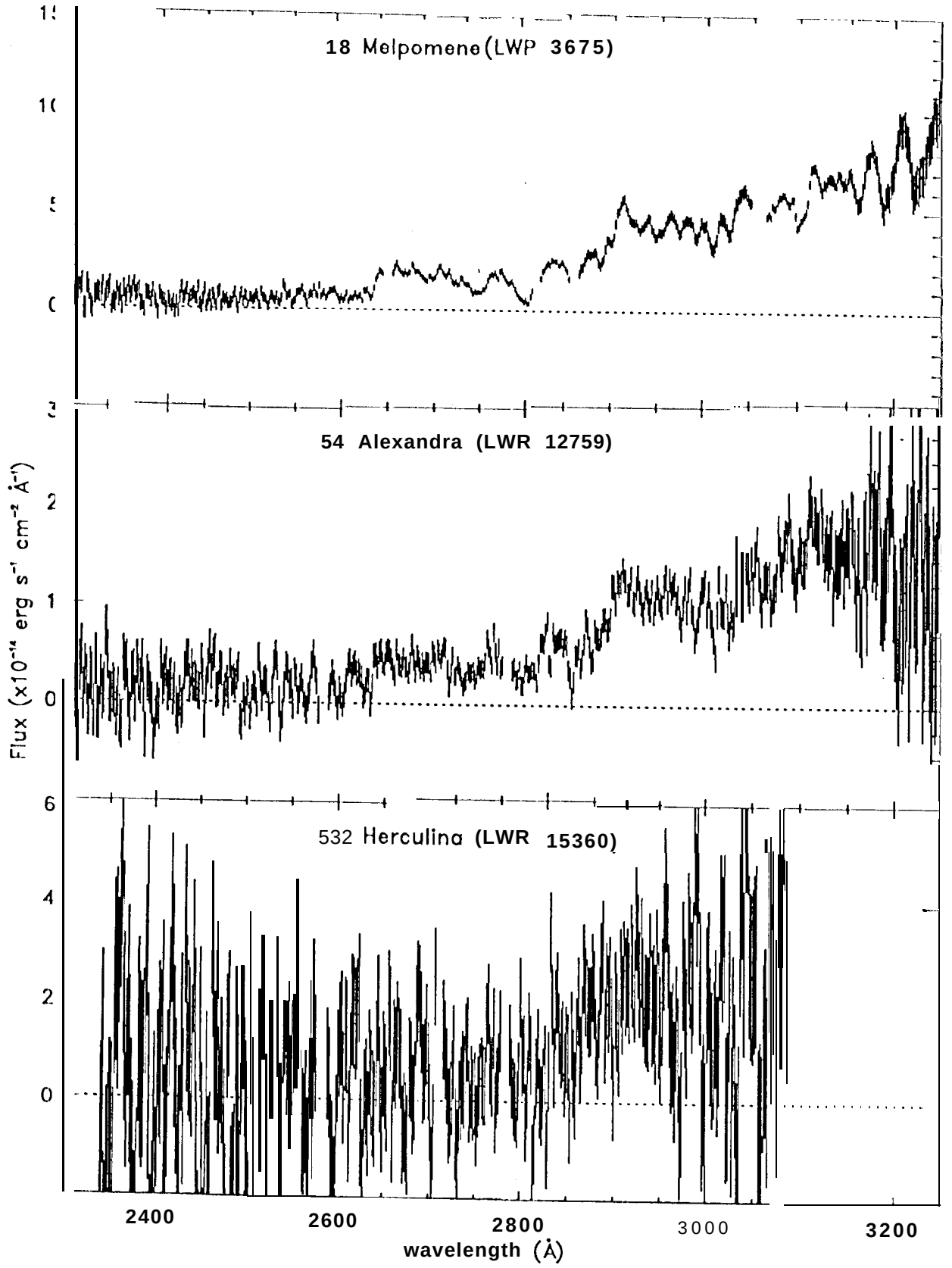

Fig 1 Roettger

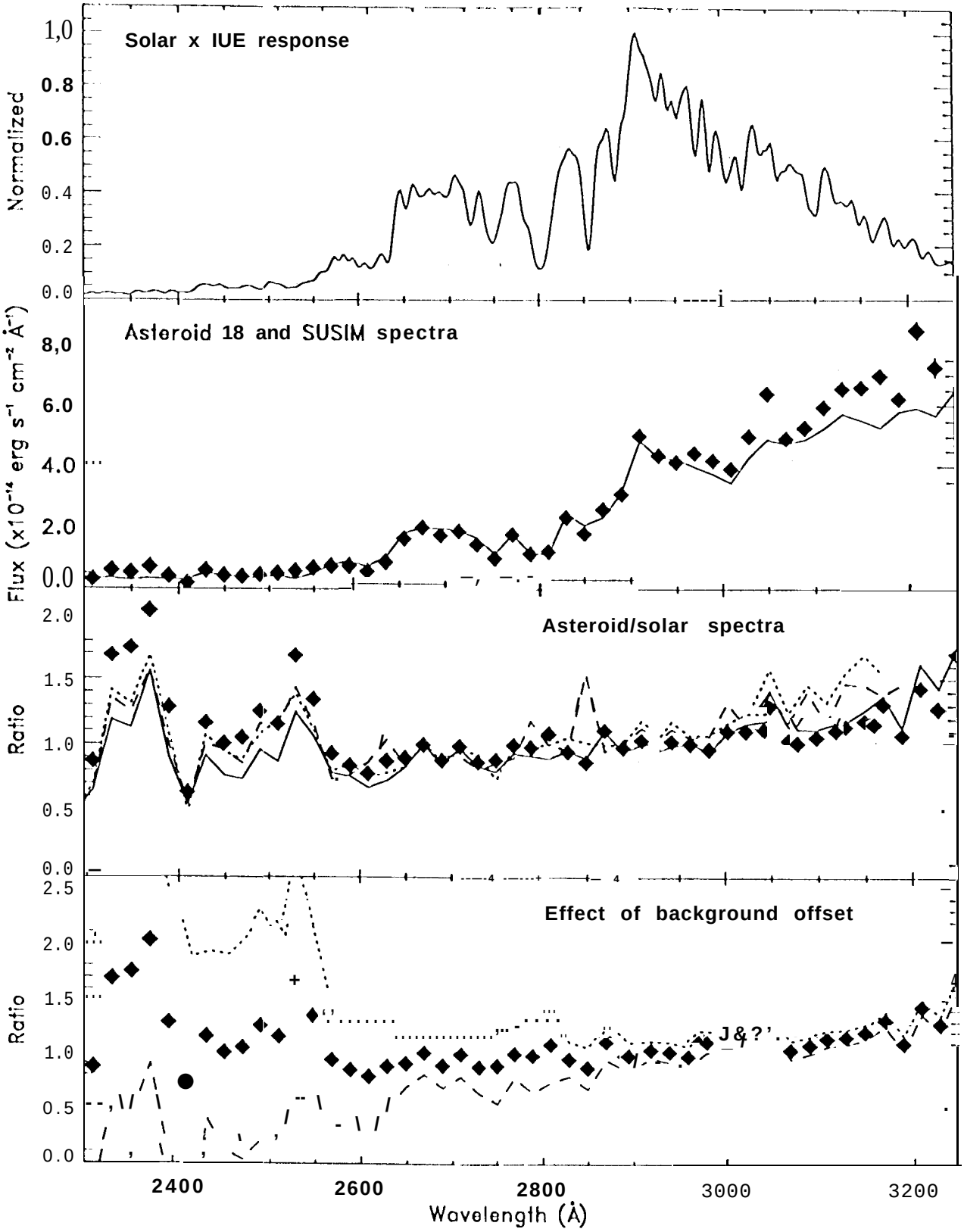

Fig 2 Roettger

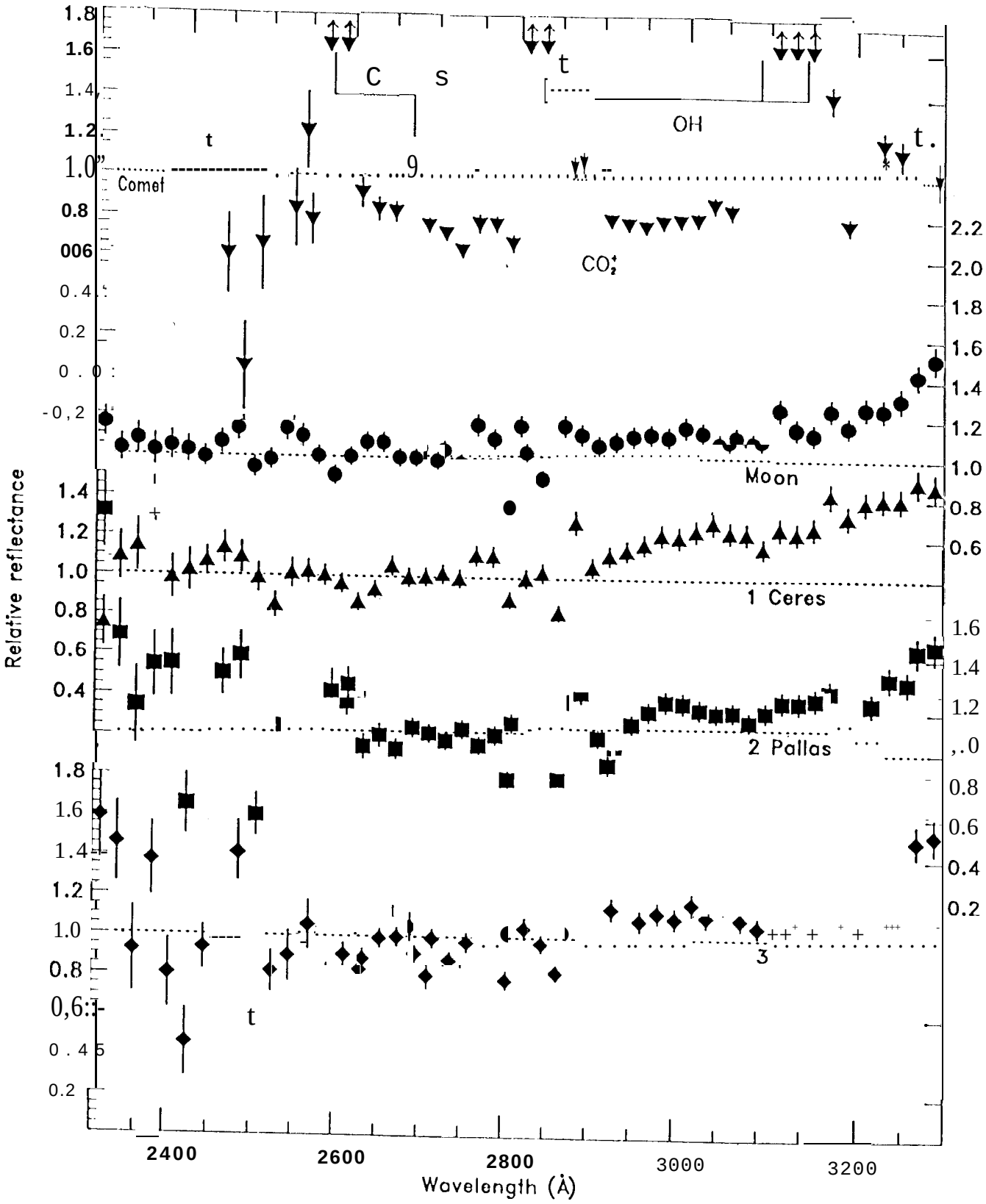

Fig 30 Roettger

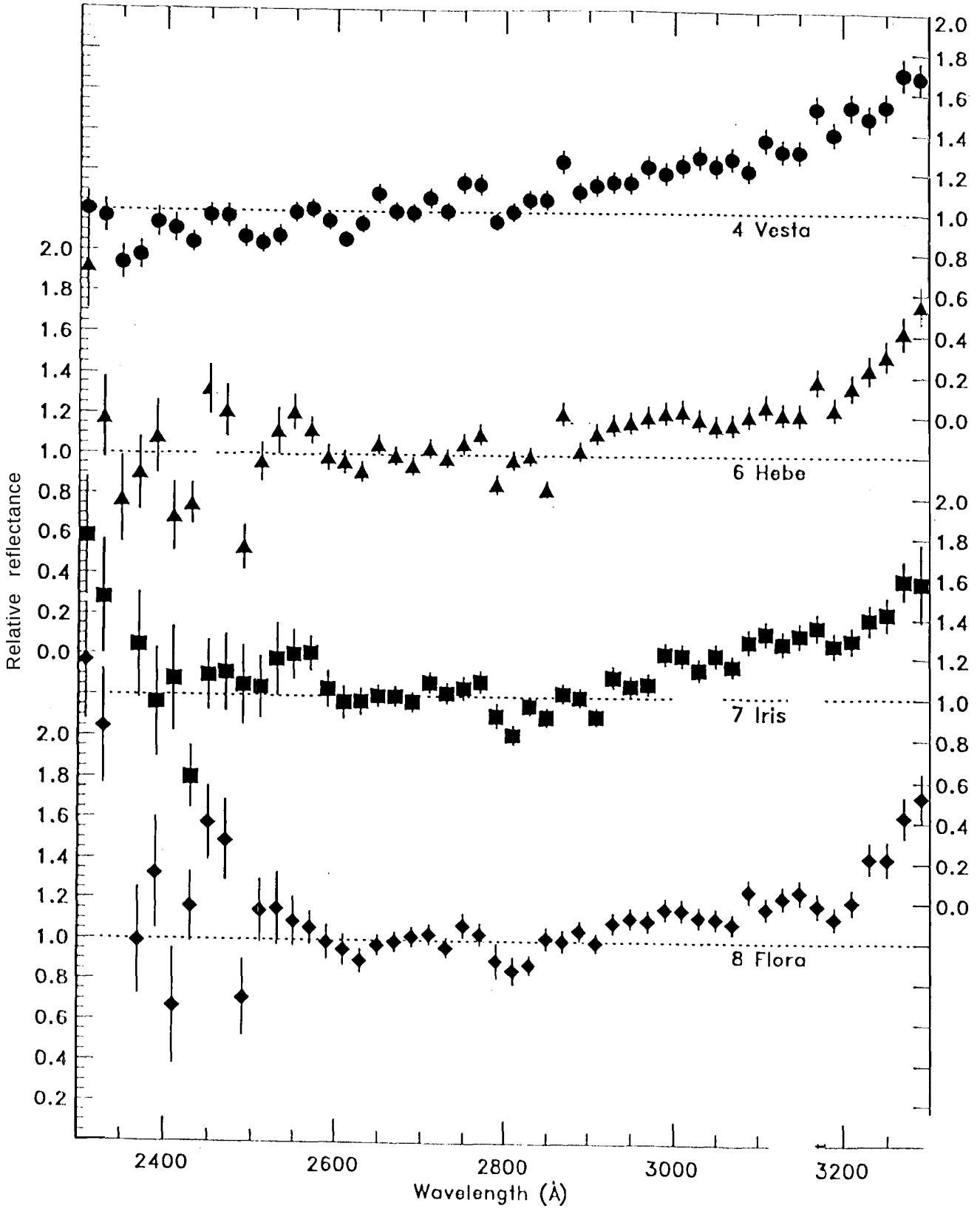

Fig 3b Roettger

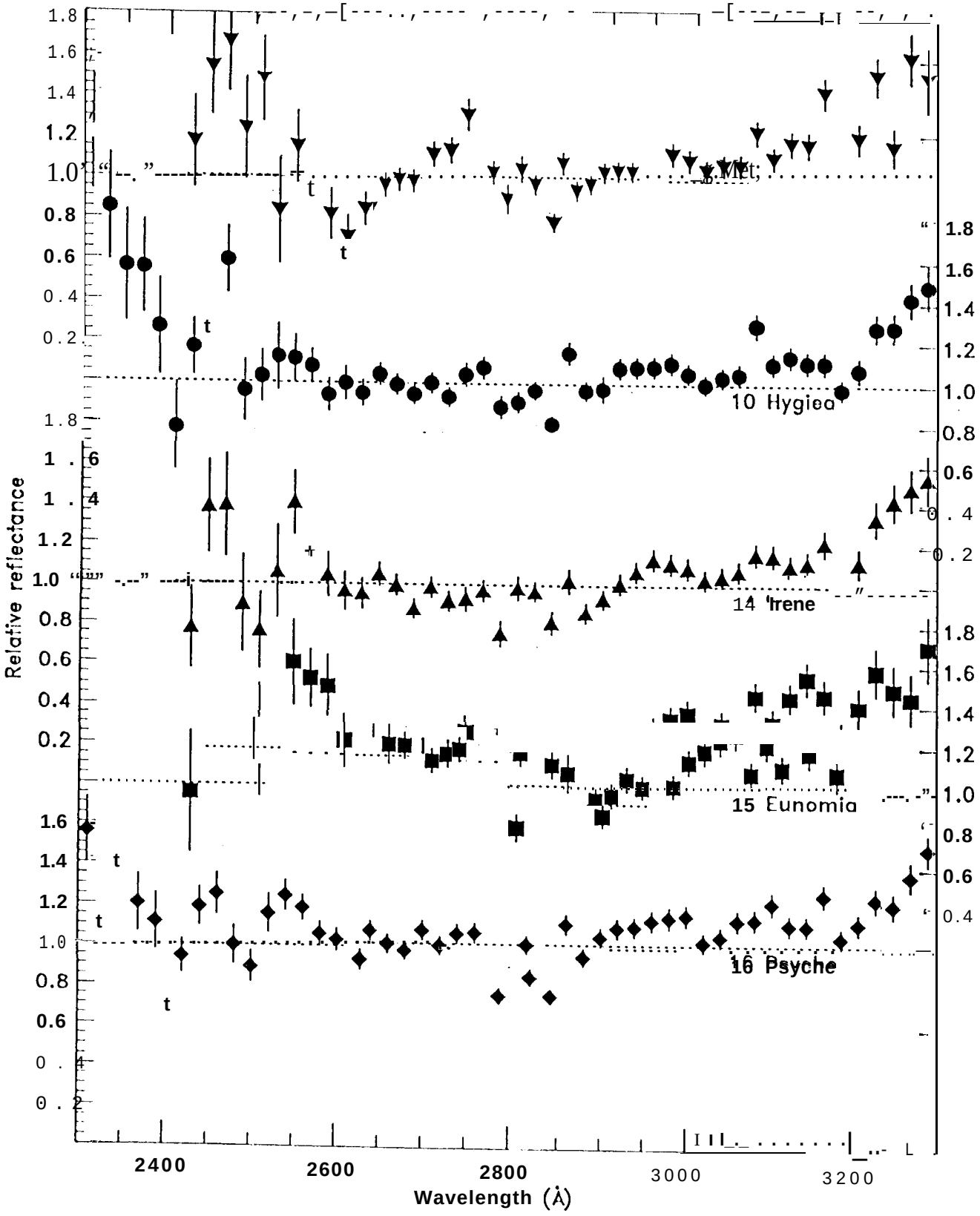

Fig 3c Roettger

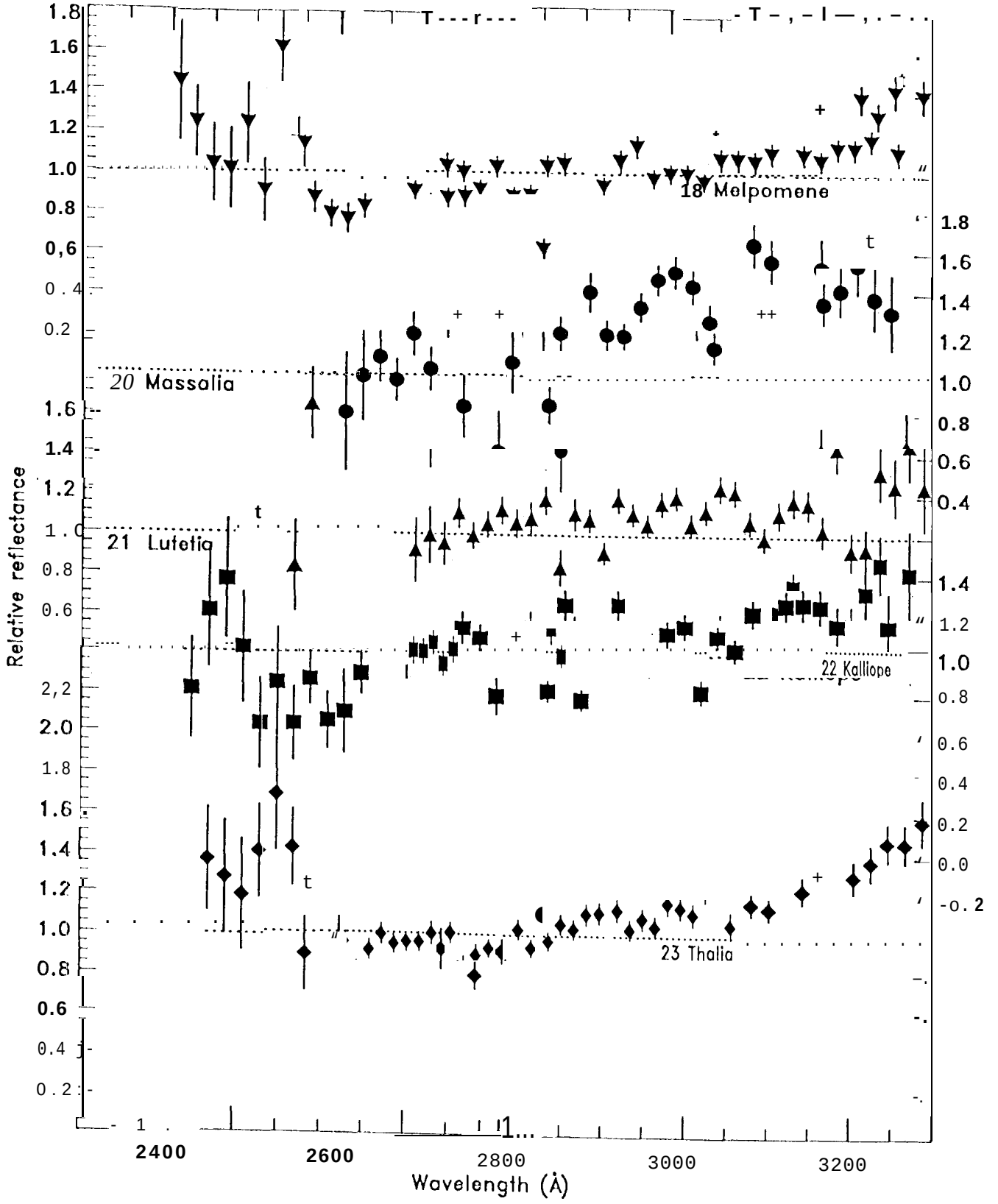

Fig 3d Roettger

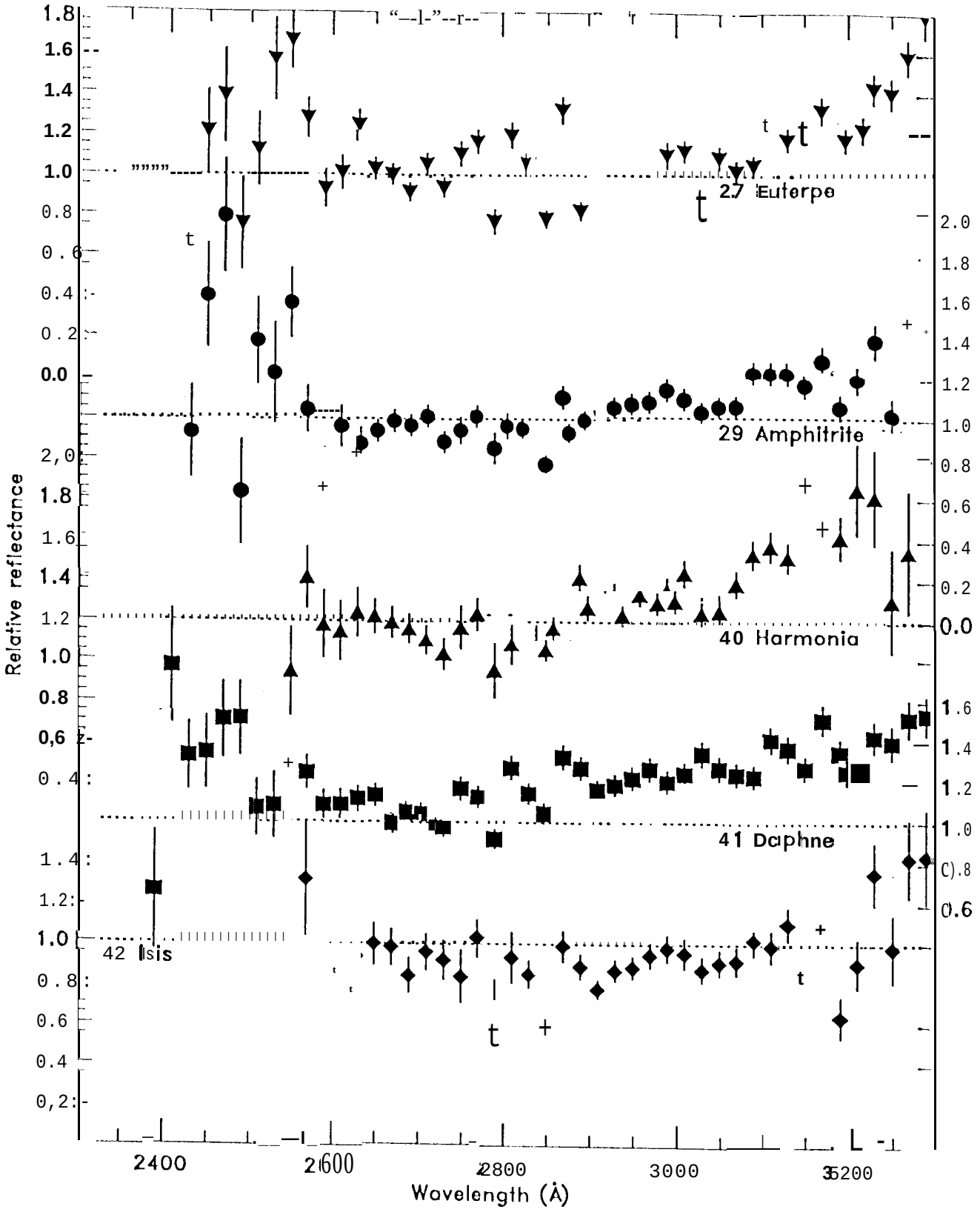

Fig 3e Roettger

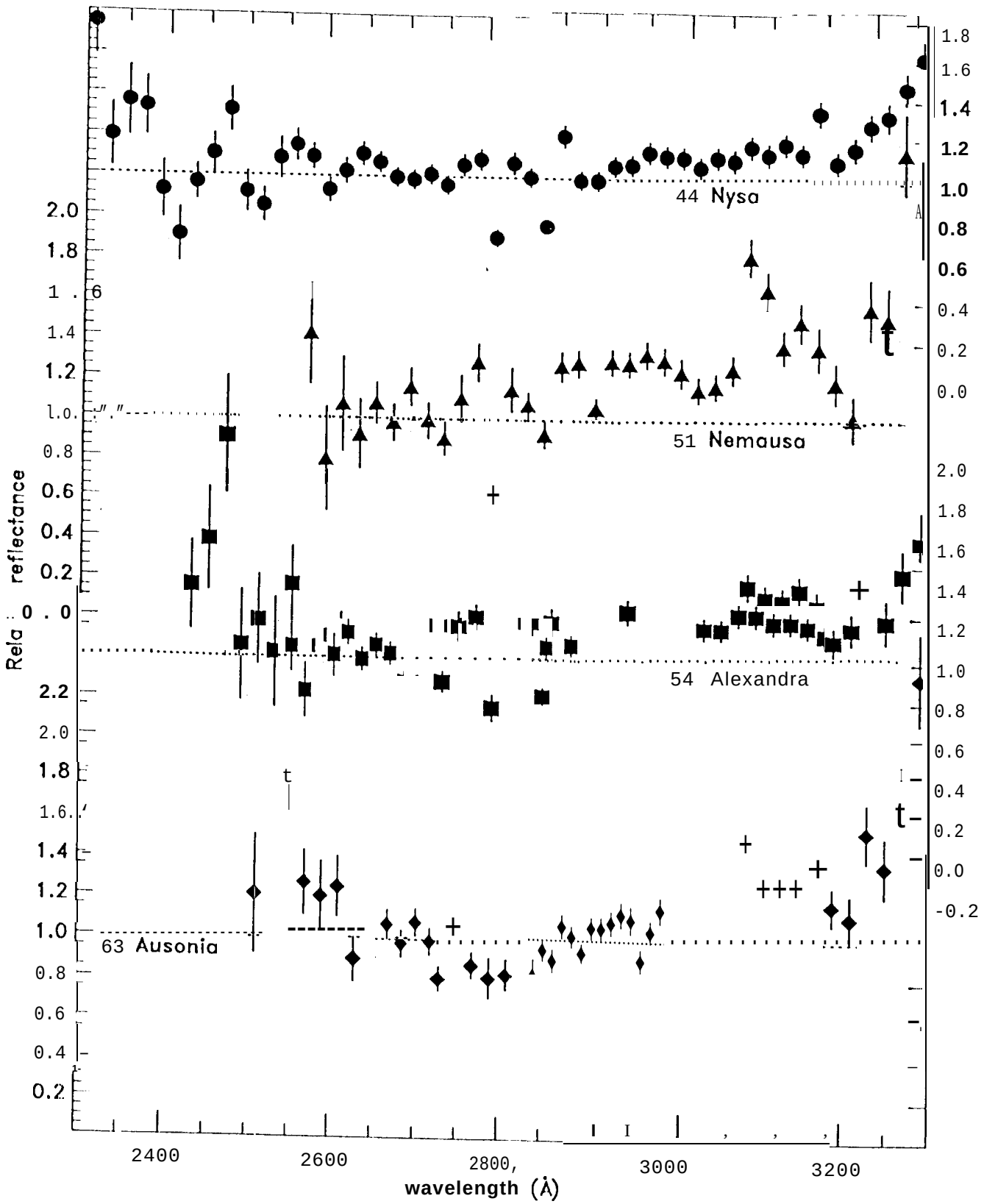

Fig 3f Roettger

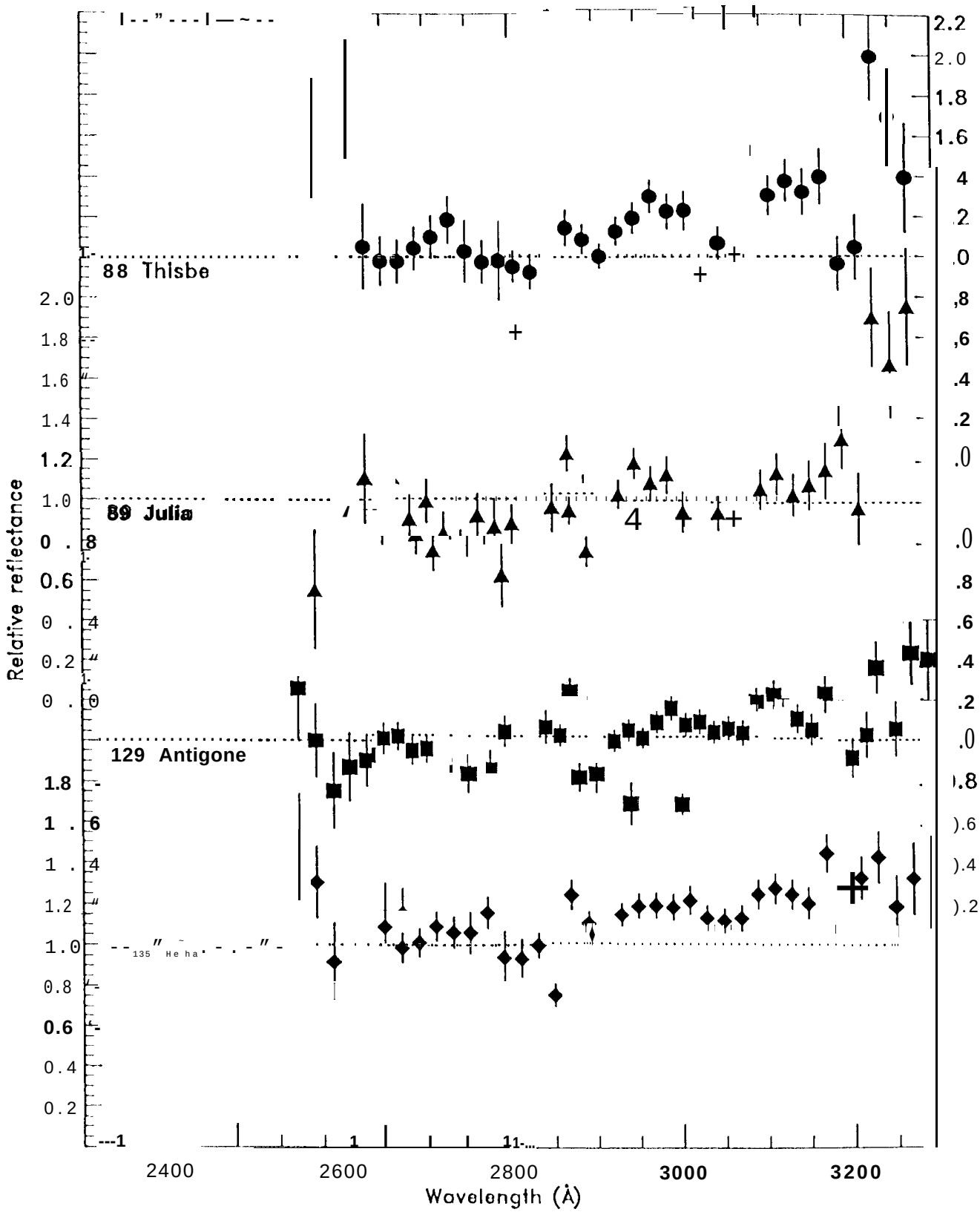

Fig 39 Roettger

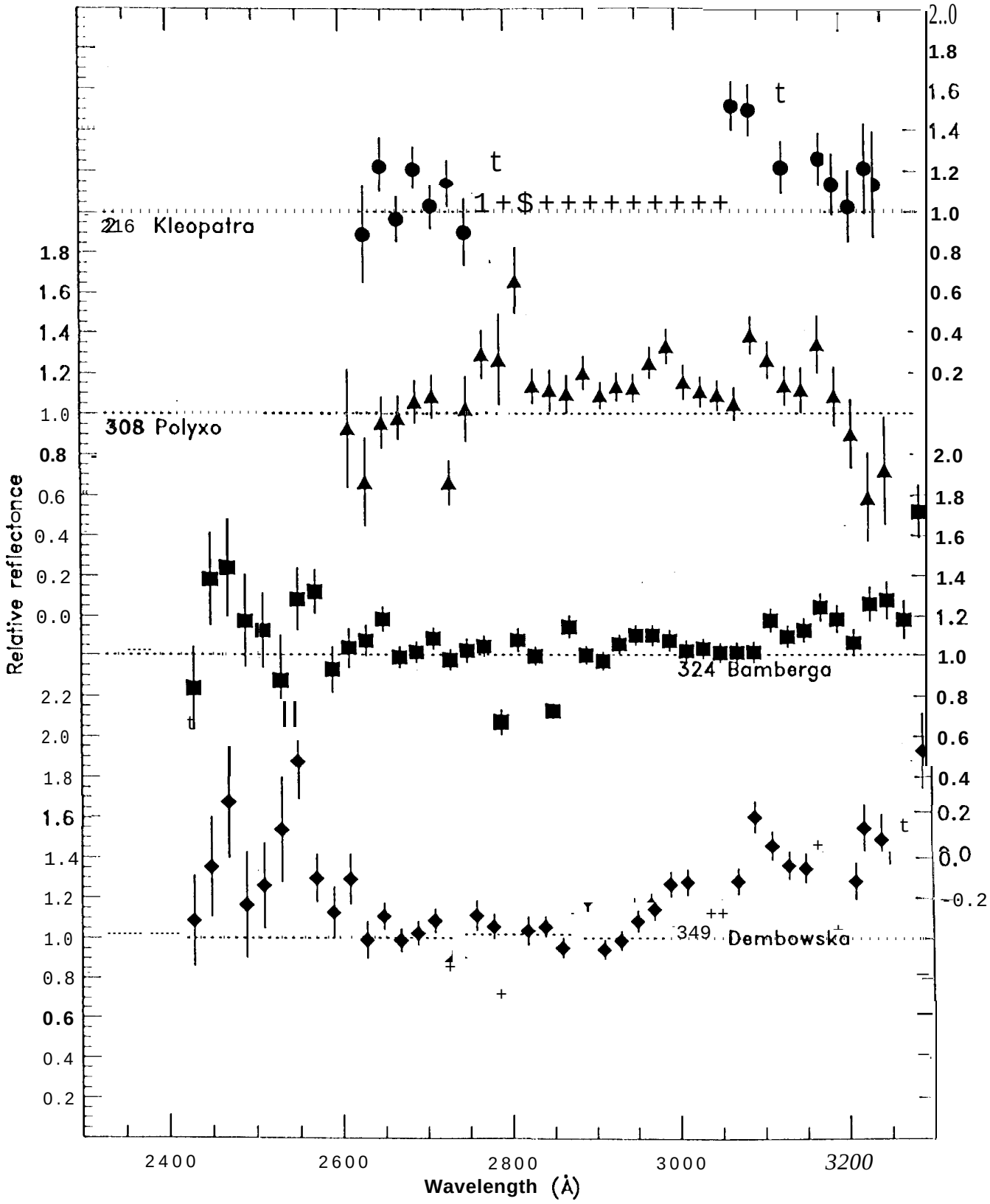

Fig 3h Roettger

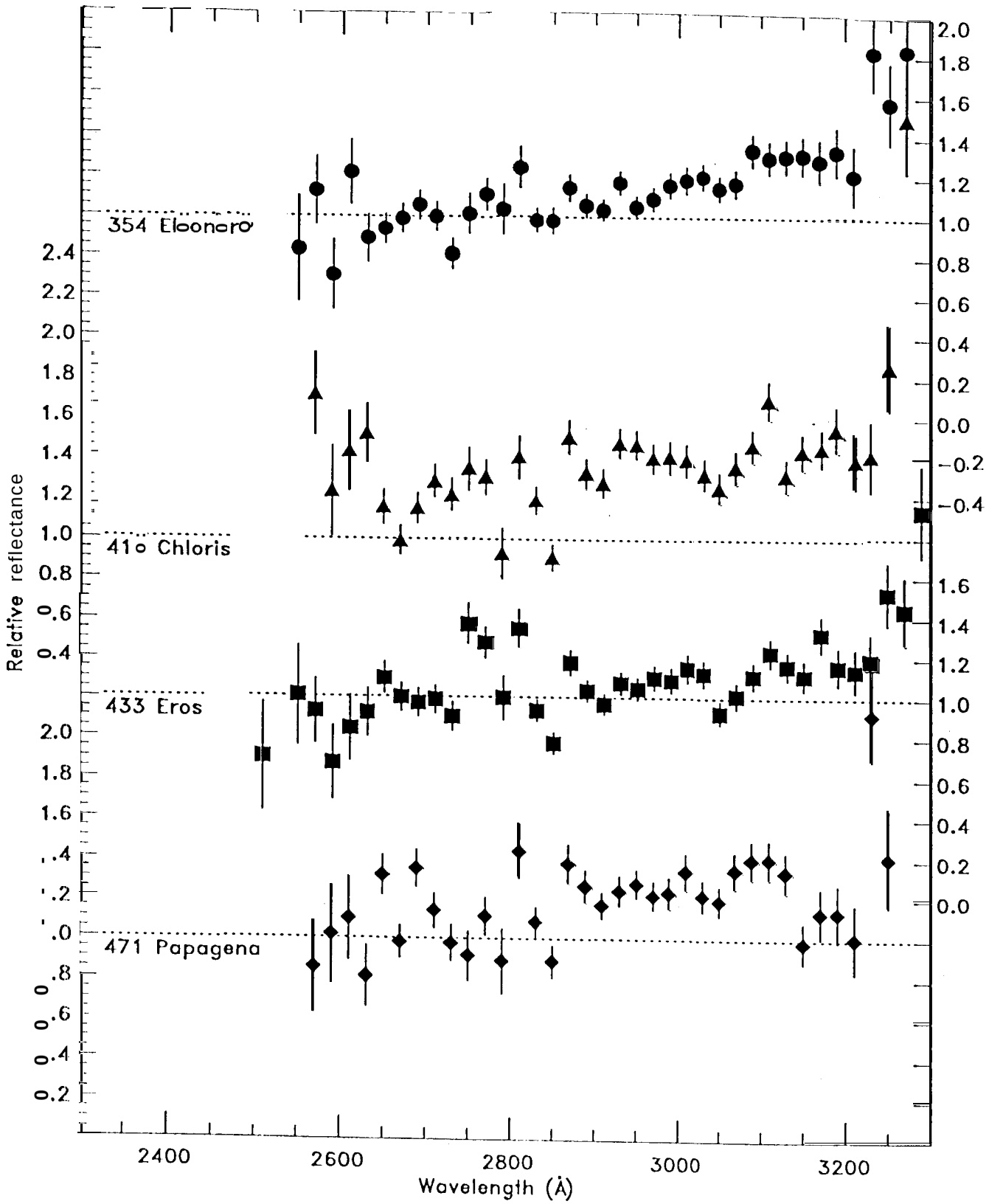

Fig 31 Boettger

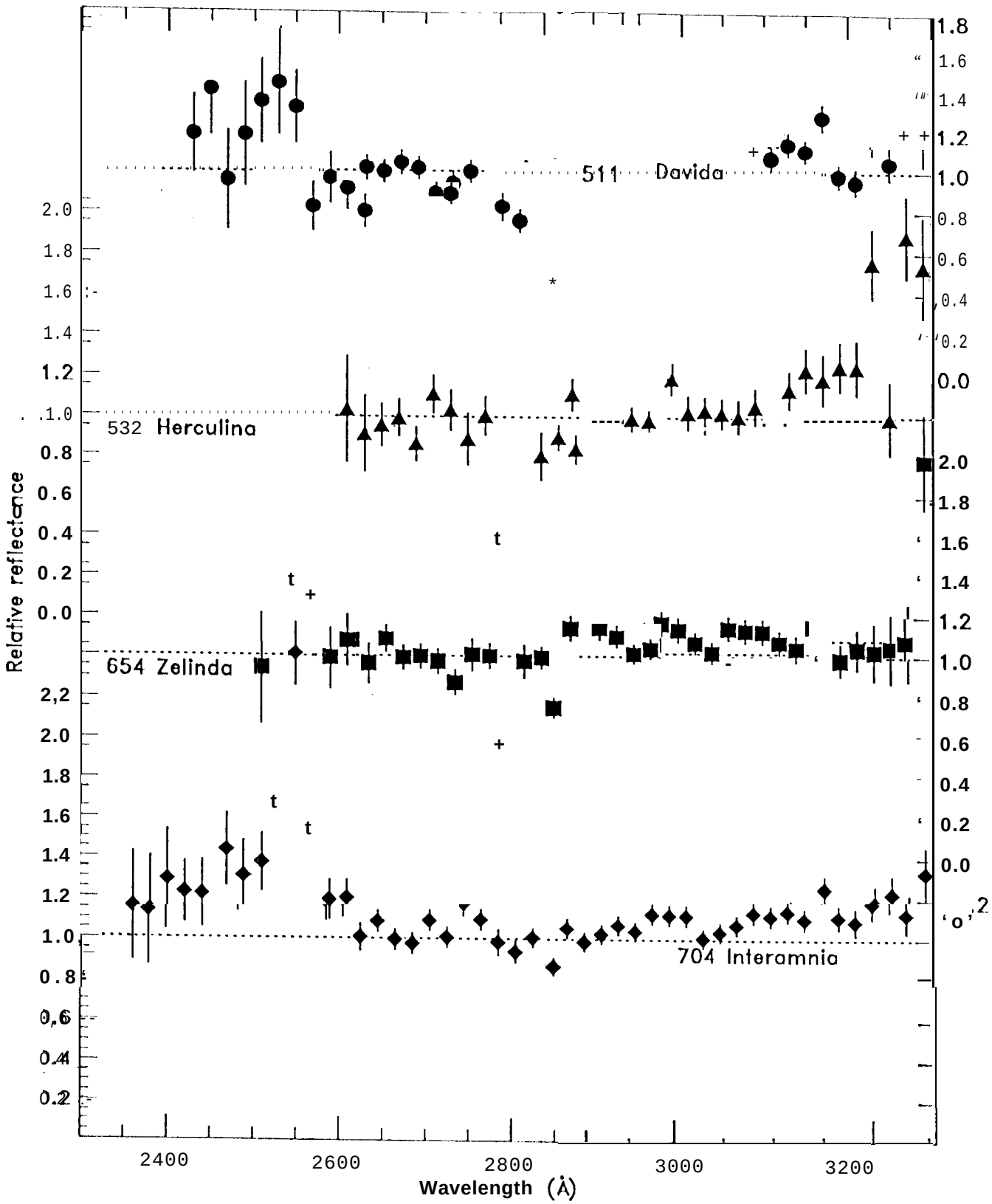

Fig 3| Roettger

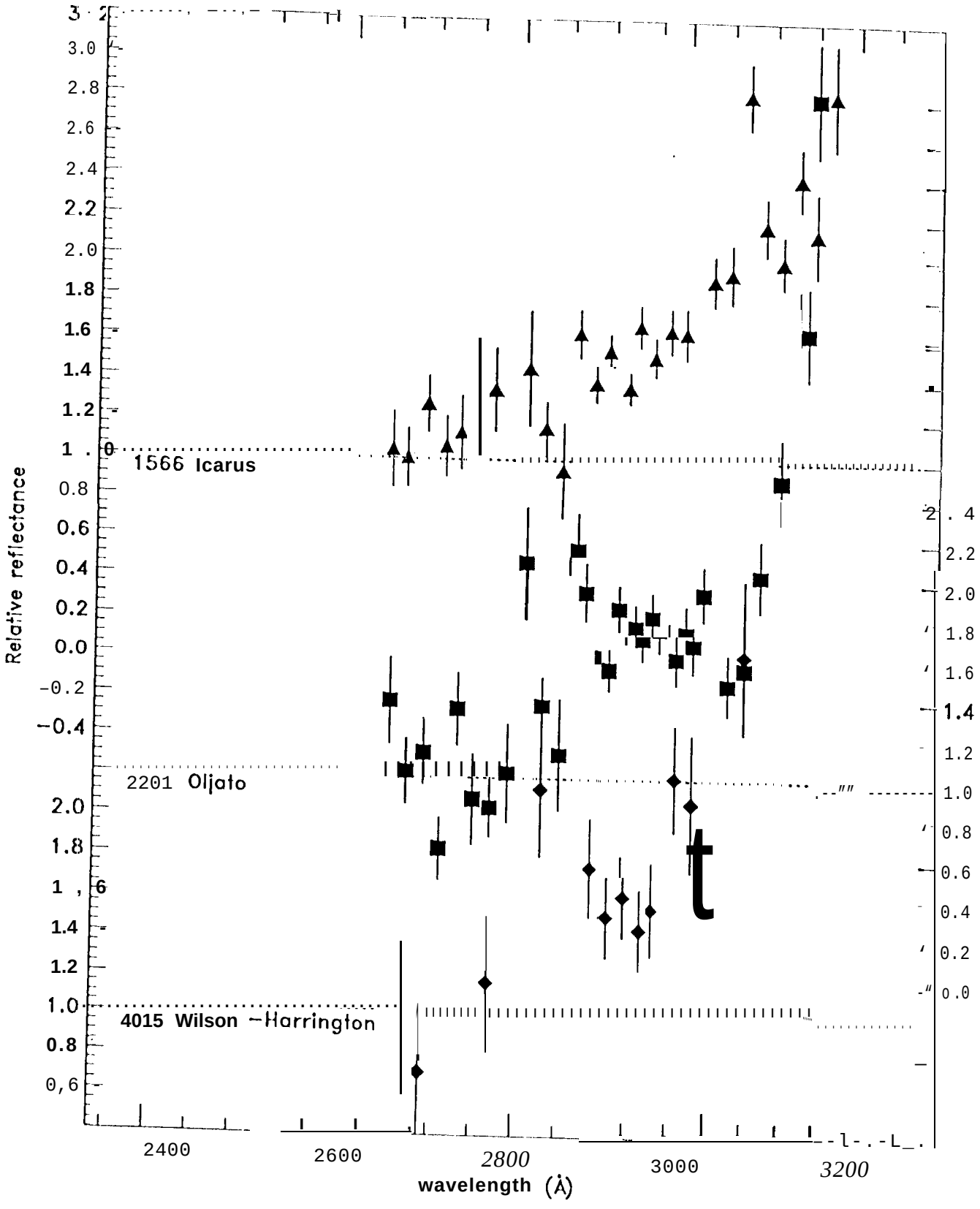

Fig 3k Roettger

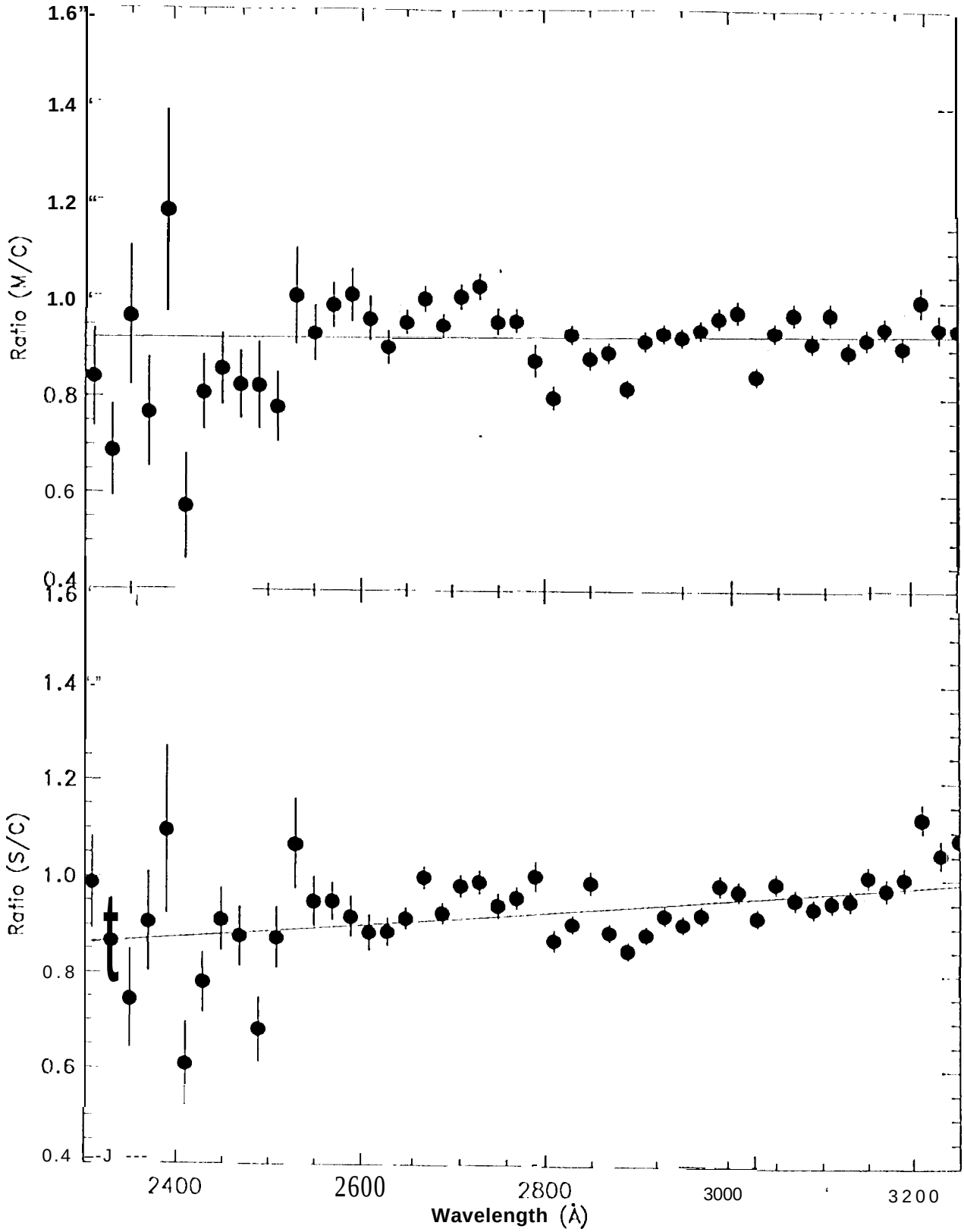

Fig 4 Roeltger

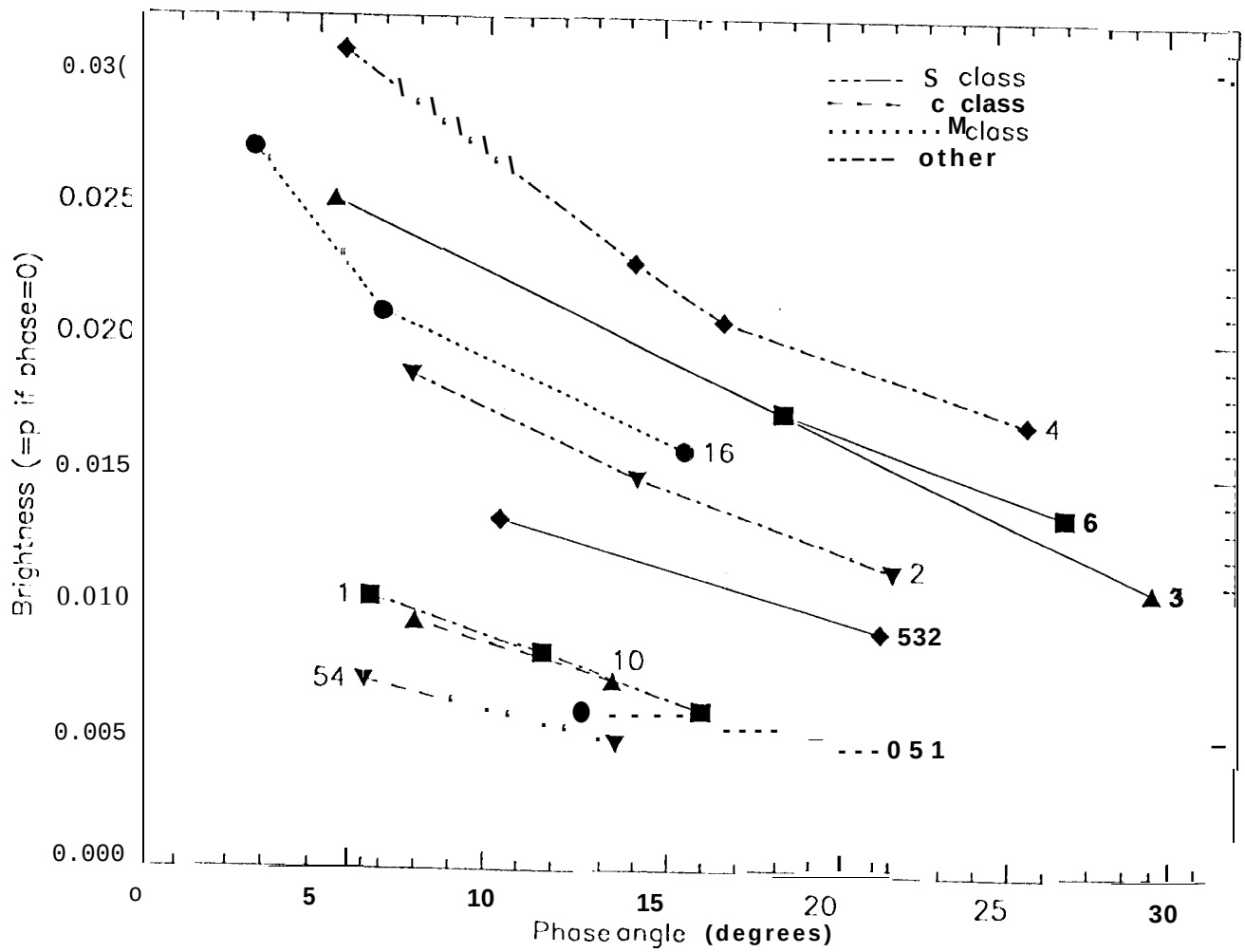

Fig 5 Roettger

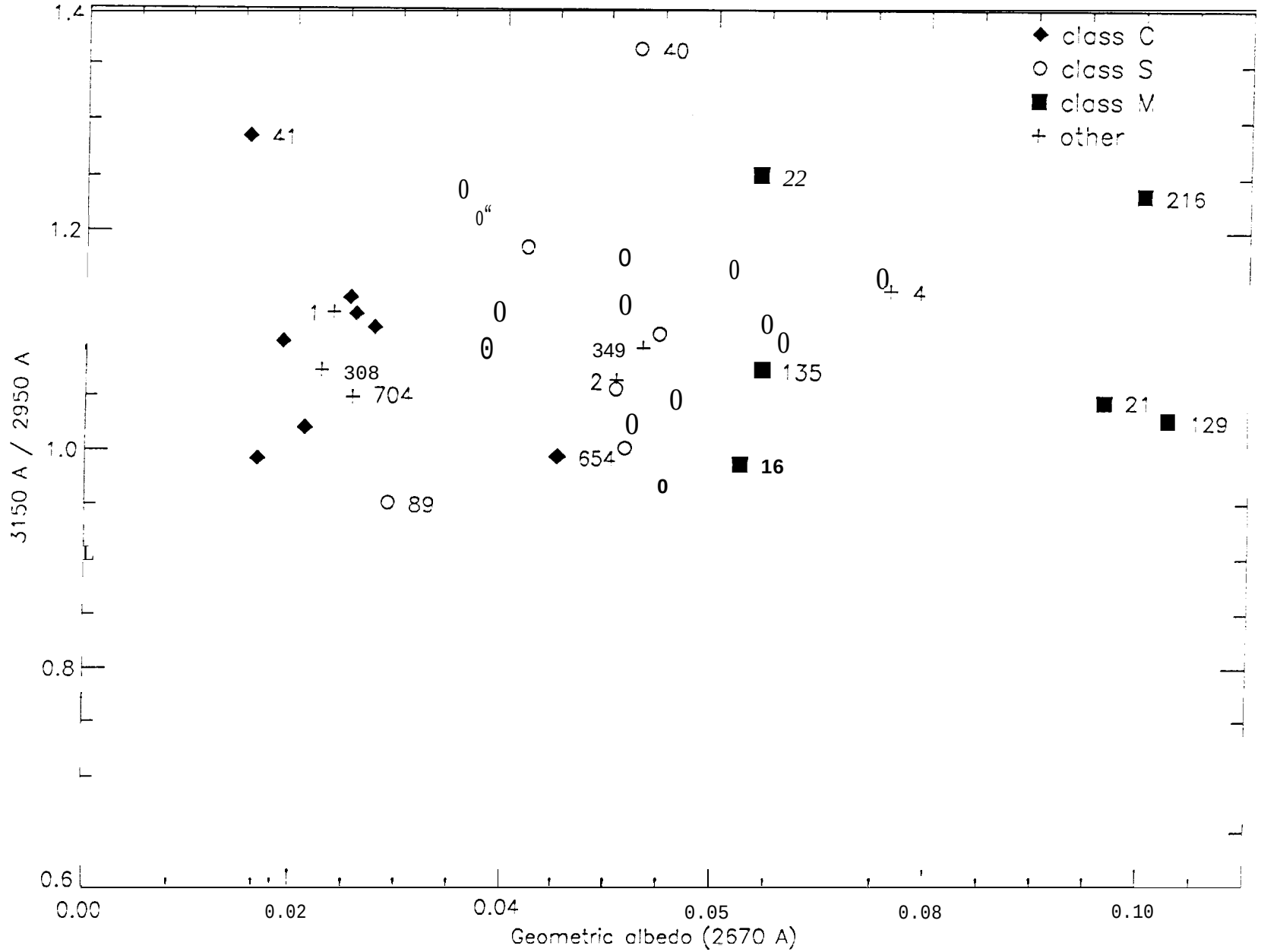

Fig 6 Roettger